Institute of Solid State Physics
University of Latvia

ANNUAL REPORT 2018

Riga 2019

Annual Report 2018, Institute of Solid State Physics, University of Latvia.
Editor: Dr.habil. phys. A.Sternbergs.
Set up at the Institute of Solid State Physics, University of Latvia,
Kengaraga Str. 8, LV-1063, Riga, Latvia.

Riga, Institute of Solid State Physics, University of Latvia, 2018, p.64

Director: **Dr. phys. M.Rutkis**
Institute of Solid State Physics, University of Latvia
Kengaraga Str. 8, LV-1063 Riga, Latvia
***Tel.:** +371 67187816*
***Fax:** +371 67132778*
ISSP@cfi.lu.lv
http://www.cfi.lu.lv

Contents

Introduction

The research in solid state physics at the University of Latvia restarted after World War II. The Institute of Solid State Physics (ISSP) of the University of Latvia was established on the basis of Laboratory of Semiconductor Research and Laboratory of Ferro- and Piezoelectric Research in 1978. Since 1986 the ISSP has the status of an independent organization of the University and now is the main material science institute in Latvia.

Four laboratories from the Institute of Physics of the Latvian Academy of Sciences joined our Institute in 1995. Twenty scientists of the former Nuclear Research Centre joined the ISSP in 1999 and established Laboratory of Radiation Physics. In 2004 scientists from the Institute of Physical Energetics joined ISSP and established Laboratory of Organic Materials.

In mid 90-ties the ISSP has intensified its teaching activities. A number of researchers have been elected as professors of the University of Latvia. Post-graduate and graduate curricula were offered in solid state physics, material physics, chemical physics, physics of condensed matter, semiconductor physics, and experimental methods and instruments.

In December 2000 the ISSP was awarded the **Centre of Excellence of the European Commission** (Centre of Excellence for Advanced Material Research and Technologies – **CAMART**). This honorary recognition with the accompanying financial support of 0.7 M EUR has increased our research activities, particularly extending the list of our research partners and scientists who came to work to our Institute from the leading European research centres. In 2001 the Association EURATOM-University of Latvia is established and the ISSP becomes a coordinator of the Latvian Research Unit. ISSP is leading laboratory of three associates in the Unit: The Institute of Solid State Physics, University of Latvia, Institute of Chemical Physics, University of Latvia and Institute of Physics, University of Latvia. ISSP is involved in theoretical modelling as well as experimental characterization of constructive and functional materials and has an expertise in material erosion and re-deposition in Plasma-Facing Components using Laser Breakdown Spectroscopy. In 2014 EUROfusion consortium agreement was signed, reglamenting European cooperation in thermonuclear synthesis research. In the consortium Latvia offers a deep expertise in the field of materials and in plasma-facing components. A collaboration of 34 countries aims to achieve conditions necessary for providing basis for an electricity-generating fusion power plant.

Next step of CAMART was in 2015, when ISSP won Horizon 2020 Teaming project: "**The**

Excellence Centre of Advanced Material Research and Technology Transfer – CAMART^{2}". 169 proposals were submitted, however only 31 were selected to develop their Business Plans. Between them with a score 14.5 (from 15) was the only project from Latvia submitted by the ISSP in cooperation with Swedish colleagues from the Royal Institute of Technology (KTH) and Acreo Swedish ICT. During 12 months of the Phase 1 a Business Plan for the future Centre of Excellence CAMART^{2} was elaborated, demonstrating the long - term science and innovation development strategy. Its vision is to upgrade and establish the ISSP UL as a key centre of excellence for education, science, innovation and technology transfer in the Baltic countries. Already one of Latvia's leading research institutions, the ISSP UL will become a hub for a joint collaboration and technology transfer platform for material physics based on high technologies.

The Business Plan was highly estimated in the second phase of Horizon 2020 Teaming project dedicated to the establishment of significantly stronger Centre of Excellence during 2017 – 2023.

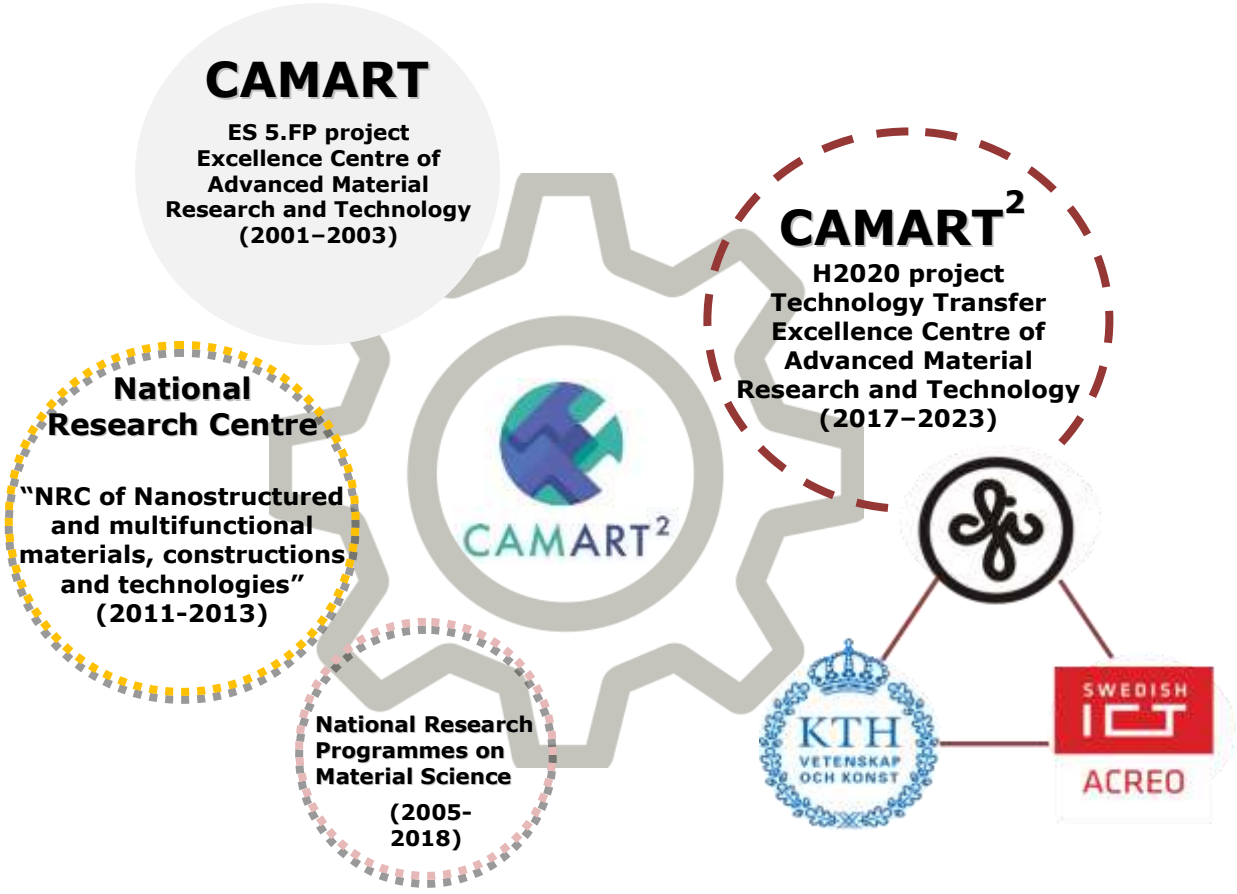

The ISSP UL is further focusing on education and undertaking an overhaul of the University's master's programme in physics to make it relevant to projected industrial needs.

Similar upgrades are also planned for the University's doctoral programme.

The ISSP UL's goal is to improve and enhance collaboration with industry in Latvia and abroad. To achieve this, it has set up a platform intended to serve as a single point of contact for scientists and companies. Named Materize, the platform provides access to the ISSP UL's expertise and resources while also facilitating communication with companies for the purpose of realising projects based on industry-specific standards. Current case studies being undertaken include a prototyping facility for cleanrooms, organic light-emitting diodes, optical lithography, vacuum deposition of thin films and composite nanomaterials synthesis.

Upon its launch in May 2018, Materize hosted its first event, the Deep Science Hackathon 2018. The Hackathon's goal was to identify high-tech ideas and find teams for their implementation, with a view to creating new products and companies that would contribute to the Baltic region's high-tech industry.

The research at the ISSP puts emphasis on four priority directions:

- Theoretical and experimental studies of materials structure and properties;
- Nanotechnology, nanocomposites and ceramics;
- Functional materials for electronics and photonics;
- Energy

These priority research directions for increasing strong international scientific capacities have been strategically established and is further elaborated and implemented within 4 interdisciplinary and inter laboratory mission-oriented Domain groups:

1. Functional material theory& modelling;
2. Sensors& actuators;
3. Photonics& micro& nanoelectronics;
4. Energy

Domains represent most current trends of material science and are developed in cooperation with partners and CAMART^2 Research& Development Council. Within Domains ecosystem for innovation in material science is being developed. Domains system is basis of the new, sophisticated project applications development concept, part of ISSP UL Research. Program. It is novel, well developed and step-by-step system for ensuring flow of highly

promising project applications. Exciting projects portfolio will attract most suitable workforce to ISSP UL.

In year 2018 the concept has already shown first results, granting 6 out of 24 projects in first Fundamental and Applied Research Projects (FARP) contest of Latvian Science Council, ensuring 25% success rate instead of 16% success ratio, average in this contest. In second FARP contest it granted 3 more projects. In European Research Development Projects contest ISSP UL got one single project and three projects in cooperation with partners: Riga Technical University, Institute of Organic Synthesis and EUROLCD Ltd.

ISSP UL is also active in project proposal development for largest European Research& Innovation program Horizon 2020. Twinning project for WIDESPREAD-03-2018 with ISSP UL as coordinator “Development Research Potential for Thin Film Nanotechnologies and Modern Characterization Techniques” was submitted and another project proposal is prepared for submitting on January 22nd 2019 for the call LC-NMBP-32-2019: Smart materials, systems and structures for energy harvesting for topic "The development of new materials and material combinations with energy harvesting and storage capabilities".

Two international conferences: “Functional Materials and Nanotechnologies” and "Developments in Optics and Communications" were organized by ISSP UL in 2018. “Functional Materials and Nanotechnologies” in October 2-5, 2018 was attended by 192 participants from 22 countries: Belarus, Estonia, Finland, France, Germany, Hungary, Israel, Italy, Kazakhstan, Lithuania, Norway, Poland, Portugal, Russia, South Africa, Sweden, Taiwan, Thailand, Ukraine United Kingdom, United States, and Latvia. 6 plenary, 19 invited and 35 oral talks were given and 114 posters were presented. Next next “Functional Materials and Nanotechnologies” conference will be held in Vilnius, Lithuania in year 2020.

The highest decision-making body of the Institute is the **Scientific Council** of 15 members elected by the employees of the Institute. Presently Dr.phys. L.Trinklere is the elected chairperson of the ISSP Council. The Council appoints director and its deputies.

The interdisciplinary research at the ISSP is performed by its highly qualified staff. At end of 2018 there were 226 employees working at the Institute (196 employees at the end of 2017). For establishing horizontal laboratories, the structure of ISSP was reorganized and at the end of 2018 is as shown in Table 2. The new structure promotes research and innovation by creating service-oriented environment, fostering openness and product-oriented research.

Table 1

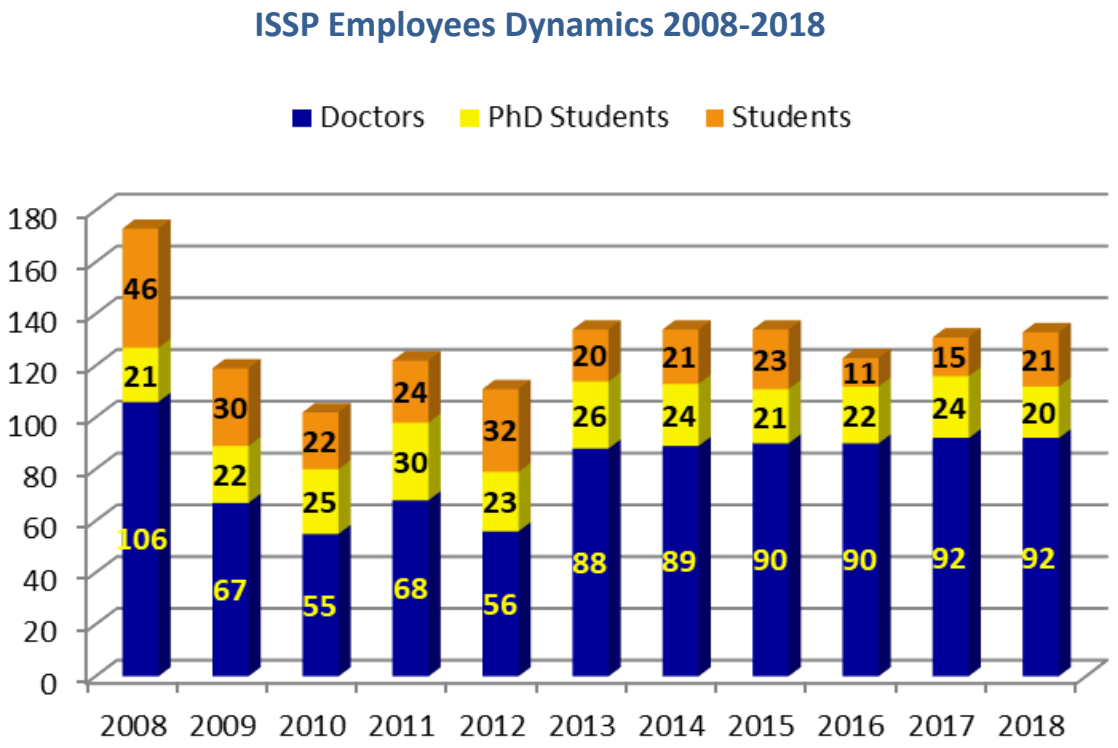

Table 2

Organisational Structure of the ISSP in 2018

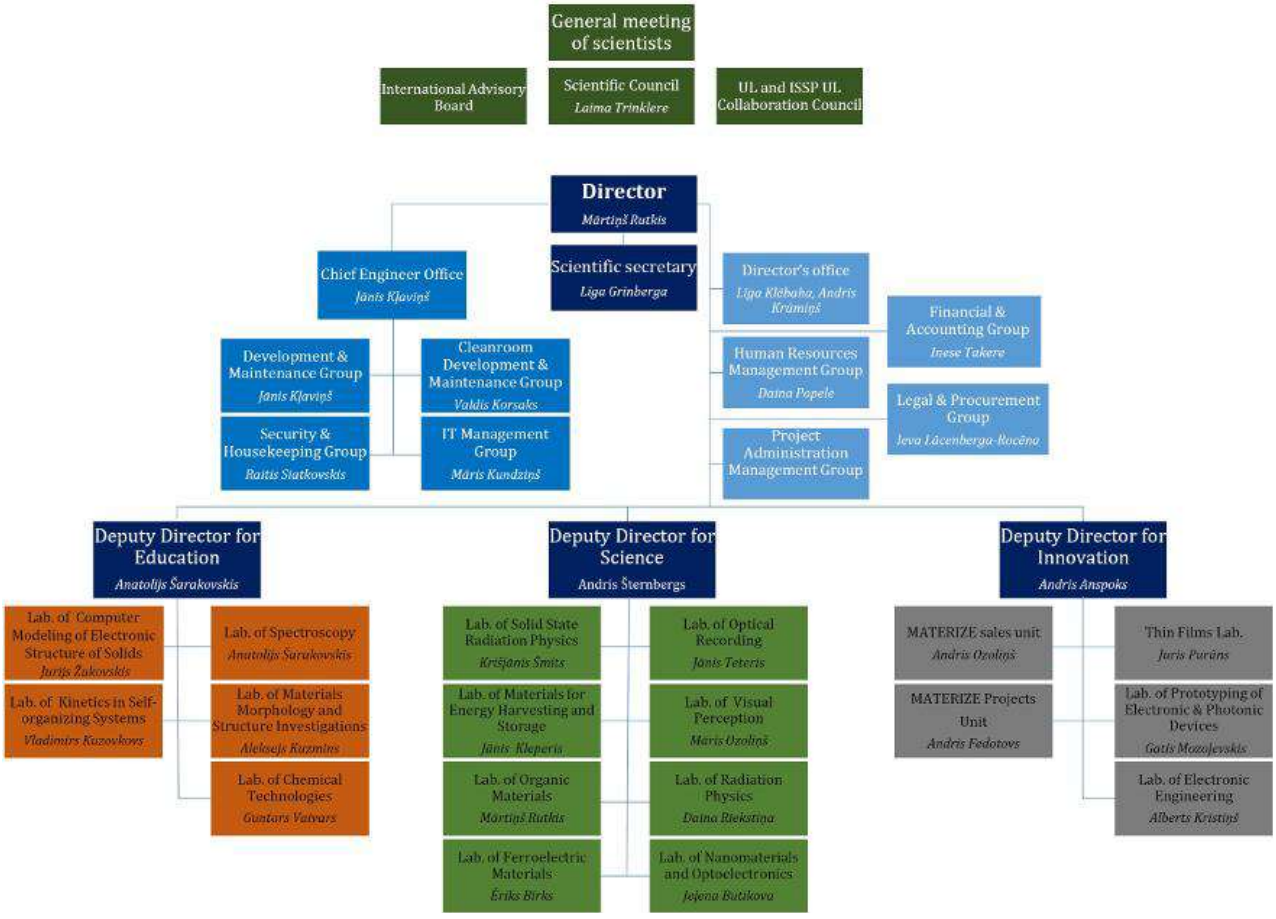

Table 3

The Scientific Council of the Institute

1. Laima Trinklere, Dr.phys., chairperson of the Council
2. Anatolijs Sarakovskis, Dr.phys.
3. Gunars Bajars, Dr.chem.
4. Jurgis Grube, Dr.phys.
5. Martins Rutkis, Dr.phys.
6. Andrejs Silins, Prof., Dr.habil.phys.
7. Donats Millers, Dr.habil.phys.
8. Andris Sternbergs, Dr.habil.phys.

9. Anatolijs Truhins, Dr.habil.phys.

10. Andris Anspoks, Dr.phys.

11. Dmitrijs Bocarovs, Dr.phys.

12. Janis Kleperis, Dr.phys.

13. Liga Grinberga, Dr.phys.

14. Marcis Auzins, Dr.habil.phys., University of Latvia

15. Maris Knite, Dr.phys., Riga Technical University

Table 4

The International Scientific Council

1. Prof. Juras Banys, Vilnius University, Lithuania

2. Prof. Antonio Bianconi, Rome International Center for Materials Science Superstripes, Italy

3. Prof. Anette Bussmann-Holder, Max-Planck-Institute for Solid State Research, Germany

4. Prof. Ming-Chi Chou, Department of Materials and Optoelectronic Science, National Sun Yat-sen University, Taiwan

5. Prof. Niels E.Christensen, Aarhus University, Denmark

6. Prof. Robert Evarestov, St.Petersburg University, Russia

7. Prof. Claes-Goran Granqvist, Uppsala University, Sweden

8. Prof. Dag Høvik, The Research Council of Norway, Norway

9. Prof. Marco Kirm, University of Tartu, Estonia

10. Dr. Jiri Kulda, Institut Laue-Langevin, France

11. Prof. Ergo Nommiste, University of Tartu, Estonia

12. Prof. Toshio Ogawa Shizuoka, Institute of Science and Technology, Japan

13. Prof. Pauls Stradins, Colorado School of Mines, USA

14. Prof. Stefan Schweizer, South Westphalia University of Applied Sciences, Germany

15. Prof. Vladimir Shur, Institute of Natural Science, Ural Federal University, Russia

16. Prof. Andrejs Silins, Latvian Academy of Sciences, Latvia

17. Prof. Sergei Tuituinnikov, Institute for Nuclear Research of the Russian Academy of Sciences, Russia

18. Prof. Juris Upatnieks, Applied Optics, USA

The annual report summarizes the research activities of the ISSP in 2018. The table No 5 below presents the key performance indicators of ISSP.

Table 5

Key performance indicators for Research	**3 years avrg.(2013-2015)**	**2016**	**2017**	**2018**	**2019 (Mid-CAMART²)**	**2023 (End of CAMART²)**	**2026 (Sustainability)**
Number of scientific publications according to "Scopus"	116	96	93	**140**	200	300	400
Fraction of scientific publications in Int. Collaboration (%)	51	74	61	**65,7**	55	60	65
Number of citations/year according to "Scopus"	1545	1908	1657	1800	2 000	2 500	5 000
Average SNIP per publications	0.790	0.748	0.896	**0.875**	1.000	1.100	1.250
Number of scientific and technical personnel (FTE)	105	113	117	**126**	130	170	180
Publications/FTE	1.11	0.85	0.79	**0.90**	1.54	1.76	2.22
Gender balance of scientific and technical personnel (% female)	26	24.5	22.2	**27.2**	30	33	37

The analysis of Key performance indicators (KPIs) is reported in the Action Plan for 2018.

Scientific Highlights

Novel method of phosphorescent strontium aluminate coating preparation on aluminum

Ivita Bite, Guna Krieke, Aleksejs Zolotarjovs, Katrina Laganovska, Virginija Liepina,
Krisjanis Smits, Krisjanis Auzins, Larisa Grigorjeva, Donats Millers, Linards Skuja
Institute of Solid State Physics, University of Latvia, LV-1063, Riga, Latvia

This study presents a novel approach to produce phosphorescent coatings on metal surfaces. Strontium aluminates are the most popular modern phosphorescent materials exhibiting long afterglow at room temperature and a broad spectral distribution of luminescence in the visible range. However, despite a large amount of research done, methods for synthesis of such materials remain relatively energy inefficient and environmentally unfriendly.

A long-afterglow luminescent coating containing SrAl2O4:Eu2+, Dy3+ is prepared by the plasma electrolytic oxidation on the surface of commercial aluminum alloy Al6082. During the electrical discharges in this process, the strontium aluminate is formed in a similar way to the solid-state reaction method. X-ray powder diffraction analysis confirms that the monoclinic SrAl2O4 phase is present in the coating.

Optical properties of the obtained coating were analyzed with luminescence methods classically used for studies of luminophores. The performance of the coating was compared with commercially available strontium aluminate powder.

The proposed method of coating synthesis may be of value for the development of energy-efficient and long-lasting automotive and public safety infrastructure.

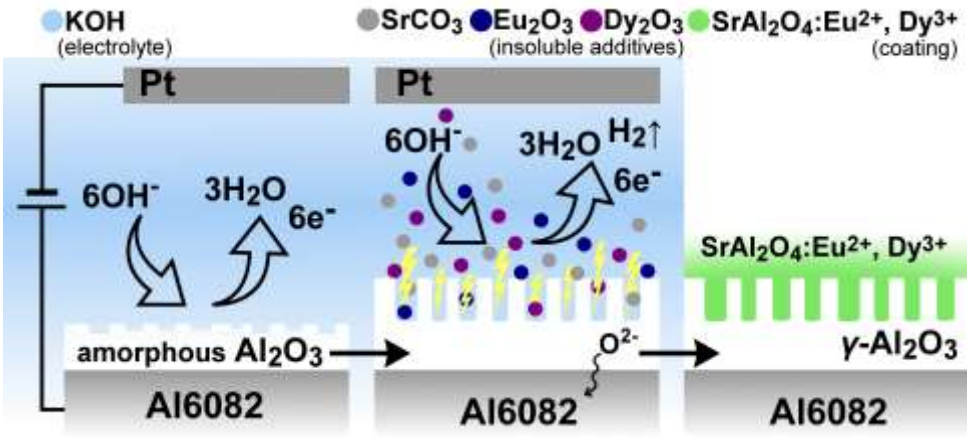

Schematic illustration of phosphorescent coating formation during PEO process

Published in:
Ivita Bite, Guna Krieke, Aleksejs Zolotarjovs, Katrina Laganovska, Virginija Liepina, Krisjanis Smits, Krisjanis Auzins, Larisa Grigorjeva, Donats Millers, Linards Skuja, Novel method of phosphorescent strontium aluminate coating preparation on aluminum, Materials and Design 160, (2018), 794–802

This work was announced by the Latvian Academy of Sciences as one the ten most significant achievements in Latvian science of the year 2018.

Theoretical and experimental studies of materials structure and properties

Domain: Computational Material Science& Modelling

Impact of point defects on the elastic properties of $BaZrO_3$: comprehensive insight from experiments and ab initio calculations.

E.A. Kotomin[1], M.F. Hoedl[2], I. Lubomirsky[3], R. Merkle[2], and J. Maier[2]

[1]*Institute of Solid State Physics, University of Latvia, Kengaraga Str. 8, LV-1063, Riga, Latvia*

[2]*Max Planck Institute for Solid State Research, Stuttgart, Germany*

[3]*Department of Materials and Interfaces, Weizmann Institute of Science, Rehovot, Israel*

Acceptor doped $BaZrO_3$ is the prototype of proton conducting perovskites which are of strong interest as electrolytes for intermediate temperature fuel cells. Elastic properties of both dry and hydrated Y-doped $BaZrO_3$ (1.5—17 mol% Y) were determined using ultrasound time of flight (TOF) measurements, and complemented by *ab initio* calculations which allow for an analysis of the different contributions. The experimental and theoretical findings are consistent and reveal a strong decrease of the Young's, shear and bulk moduli upon increasing dopant concentration. This decrease is attributed to a combined effect of (i) macroscopic lattice chemical expansion mainly caused by differing ionic radii, and (ii) presence of point defects such as acceptors $Acc Z_r$ (with decreased cation charge), oxygen vacancies VO*, and protonic defects OHO (hydroxide ions on oxide ion sites) that locally weaken the chemical bonds in the perovskite structure. The effect from modified lattice parameter is minor relative to the decrease in moduli caused by $Acc Z_r$, VO*, OHO weakening the chemical bonds. The elastic moduli differ only slightly between the dehydrated and hydrated samples. The decrease in the elastic moduli with increasing acceptor and oxygen vacancy concentrations is much stronger in Y-doped $BaZrO_3$ (-5.8% in $Y:BaZrO_3$ per mol% of vacancies) compared to similar earlier investigations on Gd-doped CeO_2 (-2% in $Gd:CeO_2$). This result indicates a greater effect of oxygen vacancies on the elastic properties in ABO_3 perovskites with the linear B—O—B bonds as compared to fluorites with strongly bent M-O-M bonds.

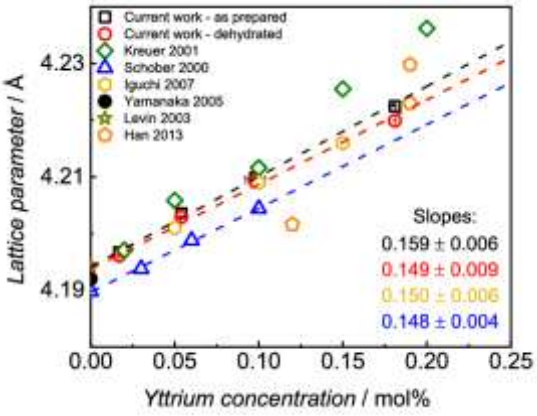

Lattice parameters of Y-doped BaZrO3 from current work and literature (Kreuer et al. pseudocubic parameter for 0.1 <x <0.2 with slight tetragonal distortion, Schober et al. , Iguchi et al., Yamanaka et al., Levin et al. ICSD 97460, Han et al. ICSD, 187800). Dashed lines are linear fits.

Published in:

M.F. Hoedl, E. Makagon, I. Lubomirsky, R. Merkle, E.A. Kotomin, and J. Maier.

Impact of point defects on the elastic properties of $BaZrO_3$: comprehensive insight from experiments and ab initio calculations. Acta Mater., 160 (2018) 247-256.*, DOI: 10.1016/j.actamat.2018.08.042 (IF=6.036, SNIP=2.737).*

Dopant solubility in ceria: alloy thermodynamics combined with the DFT+U calculations

D. Gryaznov[1], E.A. Kotomin[1], D. Fuks[2], A. Chesnokov[1], and J. Maier[3]

[1]*Institute of Solid State Physics, University of Latvia, Kengaraga Str. 8, LV-1063, Riga, Latvia*

[2]*Dept of Materials Engineering, Ben Gurion University of the Negev, Beer Sheva 84105, Israel*

[3]*Max Planck Institute for Solid State Research, Stuttgart, Germany*

Tb-doped CeO_2 (ceria) is a promising mixed conductor for oxygen permeation membranes and reversible oxygen sorbents. To predict solubility of Tb ions in ceria for a wide range of concentrations, density functional theory (DFT+U) calculations with two different values of Hubbard U-parameter on Tb and Ce ions were combined with alloy thermodynamics and the Concentration Wave approach. It is shown how to predict properties of disordered solid solutions at finite temperatures, using the energy parameters in the mixing energies extracted from the DFT + U calculations performed at T = 0 K for two ordered configurations of the dopant in the supercells. The unlimited solubility of Tb^{4+} in CeO_2 in the quasi-binary cross-section CeO_2-TbO_2 is predicted in the temperature range where both stoichiometric TbO_2 and CeO_2 reveal fluorite structures (above 700 °C).

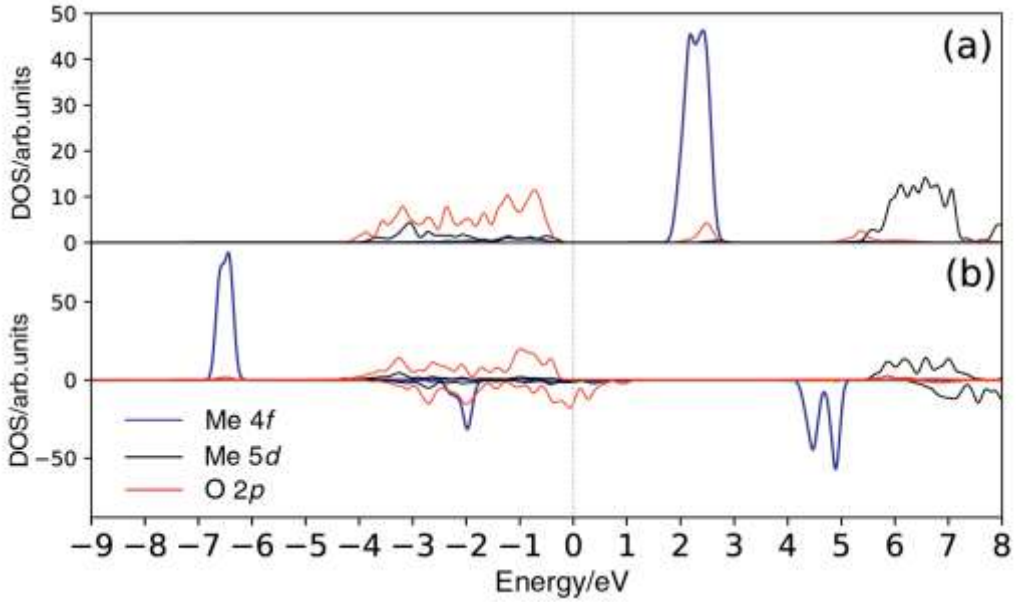

The projected density of states (DOS) for CeO2 (a) and TbO2 (b). The Fermi energy is set to zero. Notice that CeO2 is non-magnetic, and, therefore, its spin down electrons are not shown. Me stands for Ce in (a) and Tb in (b). In b) Tb *4f* peak at −2 eV was multiplied for better visibility by the factor of 4.

Published in:
D. Fuks, D. Gryaznov, E.A. Kotomin, A. Chesnokov, and J. Maier.
Dopant solubility in ceria: alloy thermodynamics combined with the DFT+U calculations.
Solid State Ionics, 325 (2018) 258–264. DOI: 10.1016/j.ssi.2018.08.019 (IF=2.751, SNIP=0.952).

Anomalous kinetics of diffusion-controlled defect annealing in irradiated ionic solids

E. Kotomin[1], V. Kuzovkov[1], A.I. Popov[1], J. Maier[2], and R. Vila[3]
[1]*Institute of Solid State Physics, University of Latvia, Kengaraga Str. 8, LV-1063, Riga, Latvia*
[2]*Max Planck Institute for Solid State Research, Stuttgart, Germany*
[3]*CIEMAT, Madrid, Spain*

The annealing kinetics of the primary electronic F-type color centers (oxygen vacancies with trapped one or two electrons) is analyzed for three ionic materials (Al_2O_3, MgO, and MgF_2) exposed to intensive irradiation by electrons, neutrons, and heavy swift ions. MgO, α-Al_2O_3 (sapphire, corundum), and MgF_2 are three wide gap insulating materials with different crystalline structures and chemical bonding. All three materials are radiation resistant and have many important applications, also in fusion reactors.

Phenomenological theory of diffusion-controlled recombination of the F-type centers with much more mobile interstitial ions (complementary hole centers) allows us to extract from experimental data the migration energy of interstitials and pre-exponential factor of diffusion. The obtained migration energies are compared with available first-principles calculations. It is demonstrated that with the increase of radiation fluence both the migration energy and pre-exponent are decreasing in all three materials, irrespective of the type of irradiation. Their correlation satisfies the Meyer−Neldel rule observed earlier in glasses, liquids, and disordered materials.The origin of this effect is discussed. This study demonstrates that in the quantitative analysis of the radiation damage of real materials the dependence of the defect migration parameters on the radiation fluence plays an important role and cannot be neglected.

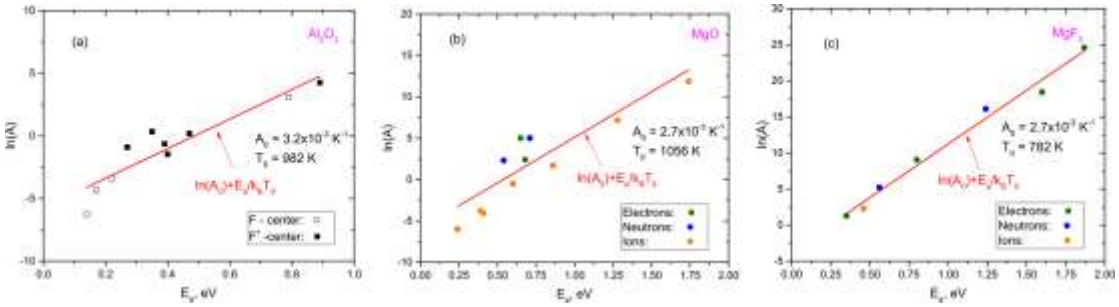

Correlation of the effective diffusion energies and pre-exponents for interstitial oxygens in sapphire (a), MgO (b), and MgF2 (c). The high quality of this correlation is characterized by the standard Pearson correlation coefficient: (a) r = 0.92819, (b) r = 0.87847, and (c) r = 0.99291, very close to the perfect case (r = 1). In all three cases the positive linear relationship takes place between the two variables.

Published in:
E. Kotomin, V. Kuzovkov, A.I. Popov, J. Maier, and R. Vila. Anomalous kinetics of diffusion-controlled defect annealing in irradiated ionic solids. J. Phys. Chem. A, 122 (2018) 28–32. DOI: 10.1021/acs.jpca.7b10141 (IF=2.836, SNIP=0.964).

Kinetic Monte Carlo modeling of Y_2O_3 nano-cluster formation in radiation resistant matrices

G. Zvejnieks, A. Anspoks, E.A. Kotomin, V.N. Kuzovkov
Institute of Solid State Physics, University of Latvia, Kengaraga Str. 8, LV-1063, Riga, Latvia

As known, Y_2O_3 nano-clusters considerably improve radiation resistance of reactor construction materials. To model the nano-cluster formation kinetics, we propose the simplest possible mathematical model nd perform kinetic Monte Carlo (KMC) simulations. We extended the KMC simulated results to the experimentally relevant times using autoregressive integrated moving average forecasting. Within the model, we have studied prototypical attractive interaction energies and particle concentrations, and compared the simulations with experiments.

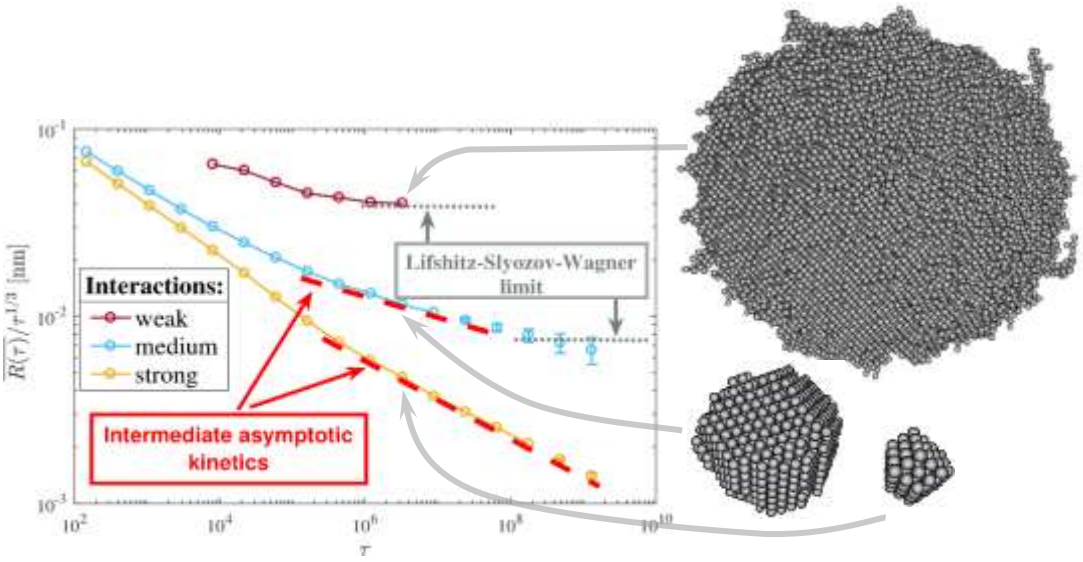

Average cluster radius growth time dependence for weak, medium and strong mutual particle attractions. Different kinetic regimes are marked with dotted and dashed lines. The characteristic clusters are shown for weak, medium and strong interactions.

We have observed the standard Lifshitz-Slyozov-Wagner (LSW) theory, predicting the average cluster radius growth with time, $R \sim t^{1/p}$, with p=3 in the long-time limit, for weak (0.1 eV) mutual particle attraction. However, the respective cluster growth rates in these KMC simulations are overestimated compared to the experiments. The best agreement with experiment is obtained for a medium (0.3 eV) and strong (0.5 eV) attractions, when nano-cluster formation occurs during *intermediate asymptotic* time scale, where power order p ranges from 5 to 7.6 depending on interaction, without reaching actually the LSW long-time limit. Such a stronger interaction leads also to a more compact {110}-faceted nano-clusters.

Published in:
G. Zvejnieks, A. Anspoks, E.A. Kotomin, V.N. Kuzovkov, Nucl. Instrum. Methods Phys. Res. B 434 (2018) 13-22. DOI: 10.1016/j.nimb.2018.08.005 (IF= 1.323, SNIP= 1.020).

Rigid versus flexible protein matrix: light-harvesting complex II exhibits a temperature-dependent phonon spectral density

M. Golub[1], L. Rusevich[2], K.-D. Irrgang[3], J. Pieper[1]
[1]*Institute of Physics, University of Tartu, W. Ostwaldi 1, 50411 Tartu, Estonia*
[2]*Institute of Solid State Physics, University of Latvia, Kengaraga 8, LV-1063, Riga, Latvia*
[3]*Department of Life Science & Technology, Laboratory of Biochemistry, University for Applied Sciences, 10318 Berlin, Germany*

Photosynthetic system of plants carries out the photosynthetic process and consists of two functionally different parts: an antenna system (light-harvesting complex, LHC) and a reaction center. LHC is large pigment-protein assembly specialized to collect solar radiation and to efficiently transfer the resulting excitation energy to photochemically active reaction center complex. The trimeric LHC of photosystem II (LHC II) is the major antenna complex of green plants (LHC II contains ~65 % of the chlorophyll associated with photosystem II).

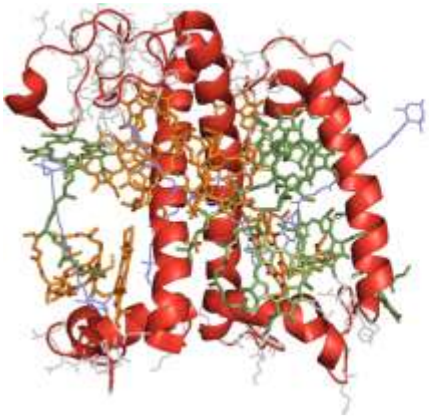

Crystal structure of the LHC II monomer.

The specific structural arrangement of pigment molecules in LHC II provides the framework for efficient, ultrafast (sub-picosecond) excitation energy transfer (EET). Although structure of LHC II is well characterized by X-ray crystallography, light harvesting and EET in these pigment-protein complexes are relatively well understood at low temperatures only (up to ~100 K). Most of the experimental and theoretical studies of EET in LHC II have been restricted to cryogenic temperatures in order that to be below the onset of conformational dynamics in proteins and calculations could be based on the static protein structure. Although EET in antenna complexes is fully functional even at very low temperatures, molecular flexibility and dynamics are essential for biological function of proteins. A number of spectroscopic properties of LHC II exhibit pronounced temperature dependences above a characteristic temperature ~120–150 K, which cannot be explained in terms of a static protein structure. Rather, such effects may point to a specific functional role of vibrational and conformational protein dynamics, which can be directly studied using inelastic and quasielastic neutron scattering (INS and QENS).

In the presented study we investigated the vibrational and conformational protein dynamics of monomeric and trimeric LHC II from spinach using INS in the temperature range of 20–305 K. The effects of the changes in protein dynamics on the spectroscopic properties of LHC II are considered in comparative model calculations. The obtained data characterize the functionally important protein vibrations in LHC II up to physiological temperatures.

Published in:
M. Golub, L. Rusevich, K.-D. Irrgang, J. Pieper, J. Phys. Chem. B 2018, 122, 7111–7121, DOI: 10.1021/acs.jpcb.8b02948 *(IF=3.146, SNIP=1.015).*

Neural network approach to EXAFS analysis

J. Timoshenko[a], A. Anspoks[b], A. Cintins[b], A. Kuzmin[b], J. Purans[b], A.I. Frenkel[a,c]
[a] *Department of Materials Science and Chemical Engineering, Stony Brook University, NY, USA*
[b] *Institute of Solid State Physics, University of Latvia, Riga, Latvia*
[c] *Division of Chemistry, Brookhaven National Laboratory, Upton, NY, USA*

The knowledge of the local atomic structure of functional materials is a key point for understanding and optimizing their properties. This task can be addressed by X-ray absorption spectroscopy, however in many practical cases the problem becomes challenging and requires the use of unconventional approaches. High-temperature phase transitions are an example of such complicated case both from experimental and theoretical sides.

In this study, an artificial neural network (ANN) approach was used to extract the information on the local structure of bulk iron and its *in-situ* temperature dependence directly from the Fe K-edge extended X-ray absorption fine structure (EXAFS) spectra. The capability of the method was demonstrated by extracting the radial distribution functions (RDFs) of iron atoms in ferritic (body-centered cubic) and austenitic (face-centered cubic) phases across the temperature-induced transition, occurring at about 1190 K.

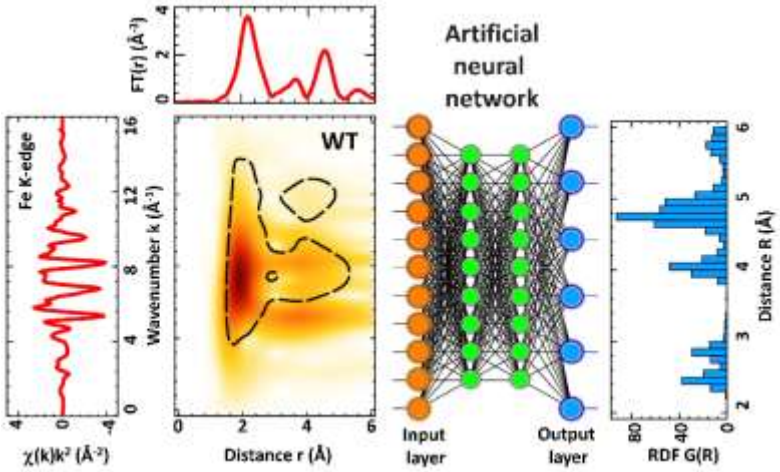

Scheme of the EXAFS spectrum analysis using the artificial neural network on the example of the Fe K-edge for bcc iron at 300 K.

The approach is based on a pre-trained ANN to convert experimentally measured EXAFS data $\chi(k)$ to the RDF $G(R)$. The important advantage of the ANN-based approach is very small computing time required to extract the RDF from EXAFS: when pre-trained ANN is available, it takes just few seconds compared to several weeks using the reverse Monte Carlo method.

The ANN approach has a wide range of possible applications for rapid analysis and real-time control of *in-situ* and *in-operando* experiments. The pre-trained ANNs can be easily shared, therefore an openly available library of ANNs can be developed in the future, allowing the researchers in the field to analyse their own data without the need to do the tedious ANN training process themselves.

This work is rated in the top 5% of all research outputs scored by *Altmetric* and has been included among Top-Stories of ELETTRA synchrotron.

Published in:
J. Timoshenko, A. Anspoks, A. Cintins, A. Kuzmin, J. Purans, A.I. Frenkel, Neural network approach for characterizing structural transformations by x-ray absorption fine structure spectroscopy, Phys. Rev. Lett. 120 (2018) 225502:1-6. DOI: 10.1103/PhysRevLett.120.225502. (IF=8.839, SNIP=2.464)

Water Adsorption on Clean and Defective Anatase TiO_2 (001) Nanotube Surfaces: A Surface Science Approach

Stephane Kenmoe[1], Oleg Lisovski[2], Sergei Piskunov[2], Dmitry Bocharov[2], Yuri F. Zhukovskii[2], and Eckhard Spohr[1]

[1]*Department of Theoretical Chemistry, University of Duisburg-Essen, Essen, Germany*

[2]*Institute of Solid State Physics, University of Latvia, Kengaraga Str. 8, LV-1063, Riga, Latvia*

Photocatalytic water splitting is considered as a clean and environmentally responsible way of satisfying global energy demands. For this purpose, the ability of different photocatalysts to drive the water splitting reaction under sunlight illumination has been studied.

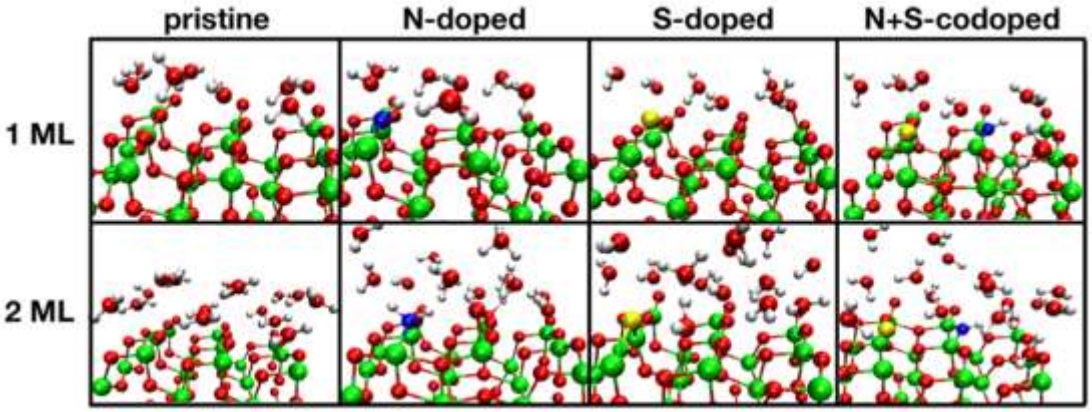

Snapshots of equilibrium trajectories for the pristine, Ndoped, S-doped, and N+S-codoped nanotube surfaces covered with a single (top row) or two monolayers of water (bottom row).

Our molecular dynamics simulations show that on the defectfree anatase TiO_2 (001) nanotube surface water adsorbs molecularly via weak interactions with the Ti sites and hydrogen bonds to surface oxygens. This binding mode is a consequence of strain-induced curvature effects, as our investigations have shown that neither the nanostructuring by slab thickness reduction nor solvation of thin planar TiO_2 (001) films alters the surface chemistry of the partially dissociated contact layer. The water molecules form a relatively strong hydrogen bond network, both for a buckled monolayer and for a multilayer-like (2 ML) film. While doping with sulfur, at the atom fraction (1/18) studied, weakens the interactions between the surface and water, nitrogen doping renders the surface more reactive to water, with a proton transfer to the surface and the formation of an NH group at the N site taking place in every studied case. At 2 ML coverage, even a second surface-assisted proton transfer takes place within the water film, resulting in the formation of an OH^- group and an NH_2ion on the surface. This effect is present only in the absence of sulfur codoping, due to the generally weaker water−nanotube interactions. The consequences of this behavior for the density of excited states will have to be investigated in a forthcoming publication.

Published in:

S. Kenmoe, O. Lisovski, S. Piskunov, D. Bocharov, Yu.F. Zhukovskii, and E. Spohr. Water adsorption on clean and defective anatase TiO_2 (001) nanotube surfaces: A surface science approach. J. Phys. Chem. B, 2018, 122, pp. 5432-5440. DOI: 10.1021/acs.jpcb.7b11697 SNIP(2017)=1.015, IF(2017)=3.146

Site symmetry approach applied to the supercell model of $MgAl_2O_4$ spinel with oxygen interstitials: Ab initio calculations

Robert A. Evarestov[1], Alexander Platonenko[2], Yuri F. Zhukovskii[2]
[1]*Institute of Chemistry, St. Petersburg State University, 198504 Petrodvorets, Russia*
[2]*Institute of Solid State Physics, University of Latvia, Kengaraga Str. 8, LV-1063, Riga, Latvia*

Ternary spinel-type AB_2O_4 oxides known and studied for a rather long time belong to the class of advanced compounds with various electrical, magnetic and optical properties. Spinel-structured magnesium aluminate ($MgAl_2O_4$), both single-crystalline and ceramic, characterized by cubic close-packed spatial crystalline morphology, possesses high transparency from visible to infrared wavelength range, enhanced strength and increased melting temperature, excellent chemical and radiation resistance as well as low electrical losses.

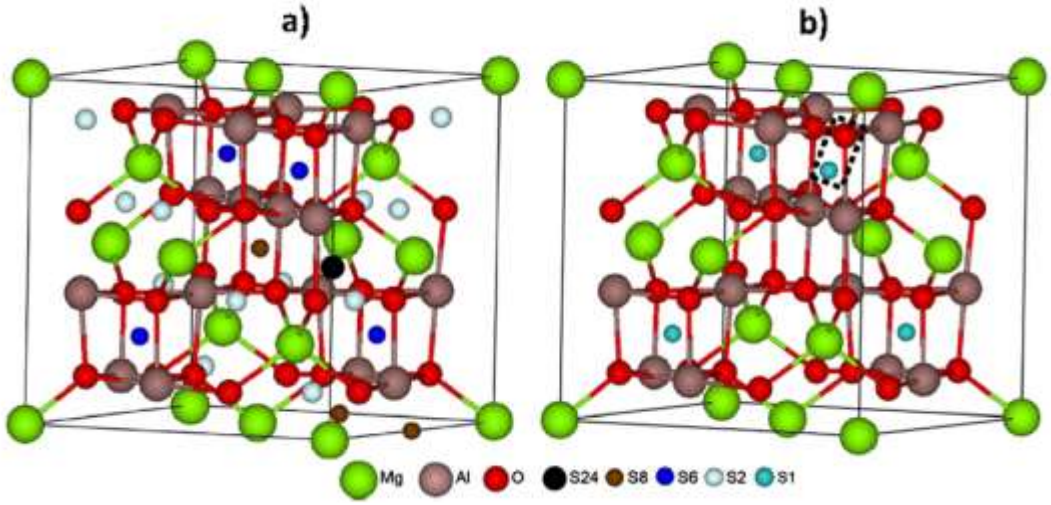

Axonometric views of L4 conventional unit cell for $MgAl_2O_4$ spinel bulk containing: (a) labeled positions of site symmetry imaged by smallest balls of different colors (S24, S8, S6 and S2); (b) interstitial S1 sites occupied the same positions as S6 ones but after total distortion of their symmetry (C1), while dotted rectangle images one of possible dumbbell orientations.

The site symmetry approach applied for various configurations of a neutral O_i interstitial per L4 and L8 supercells of $MgAl_2O_4$ spinel is based on the group-theoretical analysis of the split Wyckoff positions in the perfect crystal. When performing this analysis, we have compared five possible spatial configurations for inserting oxygen atoms into interstitial positions of a spinel structure. As expected, the interstitial configuration, highest by symmetry in the supercell model, provides the highest formation energy, while arrangement of Oi atoms in less symmetric sites of the spinel lattice is essentially more preferable energetically values of E_{form} O_i in the former are found to be 5–6 times larger. However, the examination of the lowest symmetry sites S1 only is insufficient since the low formation energy can correspond not only to C1 symmetry, but also to a higher one (it depends also on the size and shape of a supercell).

Published in:
R.A. Evarestov, A. Platonenko, and Yu.F. Zhukovskii. Site symmetry approach applied to the supercell model of $MgAl_2O_4$ spinel with oxygen interstitials: Ab initio calculations. Comput. Mater. Sci., 2018, 150, pp. 517-523. DOI: 10.1016/j.commatsci.2018.04.007 SNIP(2017)=1.251, IF(2017)=2.530

Systematic trends in (001) surface ab initio calculations of ABO_3 perovskites

R. Eglitis and A.I. Popov
Institute of Solid State Physics, University of Latvia, Kengaraga Str. 8, LV-1063, Riga, Latvia

Surface and interface phenomena, occurring in the complex oxide materials and their nanostructures, the nature of surface and interface states, and the mechanisms of surface electronic processes are very important topics in modern solid state physics. $SrTiO_3$, $BaTiO_3$, $PbTiO_3$, $CaTiO_3$, $SrZrO_3$, $BaZrO_3$, $PbZrO_3$ and $CaZrO_3$ perovskites belongs to the family of ABO_3-type perovskite oxides, and possess a large number of industrially important applications, including charge storage devices, capacitors, actuators, as well as many others

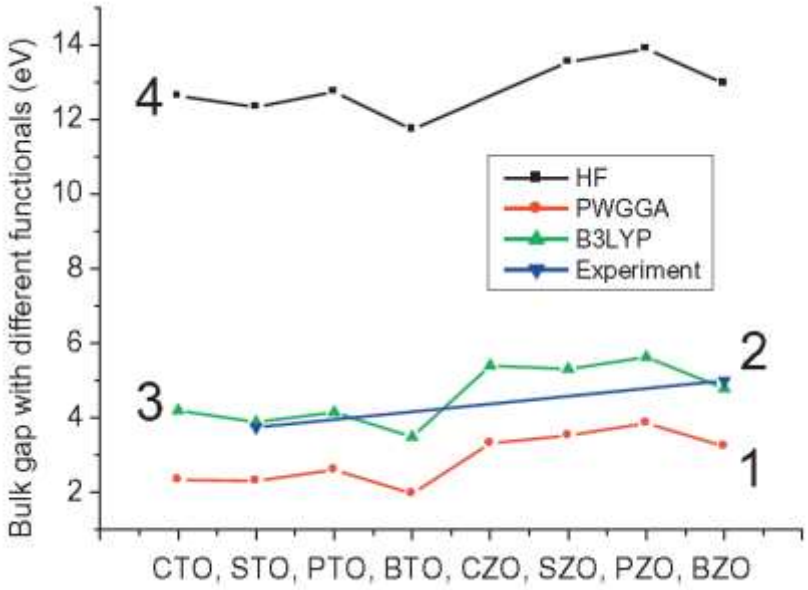

Calculated and experimental bulk C–C band gaps for eight ABO_3 perovskites obtained by means of different exchange–correlation functionals: (1) PWGGA; (2) Experiment; (3) B3LYP;(4) HF.

By means of the hybrid exchange–correlation functionals, as it is implemented in the CRYSTAL computer code, ab initio calculations for main ABO_3 perovskite (001) surfaces, namely $SrTiO_3$, $BaTiO_3$, $PbTiO_3$, $CaTiO_3$, $SrZrO_3$, $BaZrO_3$, $PbZrO_3$ and $CaZrO_3$, were performed. For ABO_3 perovskite (001) surfaces, with a few exceptions, all atoms of the upper surface layer relax inward, all atoms of the second surface layer relax outward, and all third layer atoms, again, inward. The relaxation of (001) surface metal atoms for ABO_3 perovskite upper two surface layers for both AO and BO_2-terminations, in most cases, are considerably larger than that of oxygen atoms, what leads to a considerable rumpling of the outermost plane. The ABO_3 perovskite (001) surface energies always are smaller than the (011) and especially (111) surface energies. The ABO_3 perovskite AO and BO_2-terminated (001) surface band gaps always are reduced with respect to the bulk values. The B–O chemical bond population in ABO_3 perovskite bulk always are smaller than near the (001) and especially (011) surfaces.

Published in:
R.I. Eglitis and A.I. Popov. Systematic trends in (001) surface ab initio calculations of ABO3 perovskites. J. Saudi Chem. Soc., 2018, 22, pp. 459-468. DOI: 10.1016/j.jscs.2017.05.011 SNIP(2017)=1.422, IF(2017)=2.456

Origin of pressure-induced metallization in Cu_3N: An X-ray absorption spectroscopy study

A. Kuzmin[a], A. Anspoks[a], A. Kalinko[b], J. Timoshenko[c], L. Nataf[d], F. Baudelet[d], T. Irifune[e]
[a] *Institute of Solid State Physics, University of Latvia, Riga, Latvia*
[b] *Department Chemie, Naturwissenschaftliche Fakultät, Universität Paderborn, Paderborn, Germany*
[c] *Department of Materials Science and Chemical Engineering, Stony Brook University, NY, USA*
[d] *Synchrotron SOLEIL, Saint-Aubin, Gif Sur Yvette, France*
[e] *Geodynamics Research Center, Ehime University, Ehime, Japan*

Studies of structural phase transitions driven by pressure play an important role in materials science and geosciences. Recent developments in the field have been made possible by coupling diamond anvil cells (DACs) with synchrotron radiation based techniques. Among these, X-ray absorption spectroscopy is a powerful tool to probe *in-situ* changes in the local structure of a material induced by pressure.

In this study, high-pressure (0–26.7 GPa) Cu K-edge X-ray absorption spectroscopy is used to probe possible structural modifications of anti-perovskite-type copper nitride (Cu_3N) crystal lattice. The peculiarity of the Cu_3N crystal lattice is the presence of an empty space between eight NCu_6 octahedra located at the cube corners. Such crystal lattice and its low decomposition temperature (600–800 K) indicate on the possibility of the Cu_3N structure instability under high pressure. In fact, the pressure-induced metallization of Cu_3N above ≈5 GPa has been observed in the past by electrical resistance and optical absorption measurements. However, its origin remains a puzzling task.

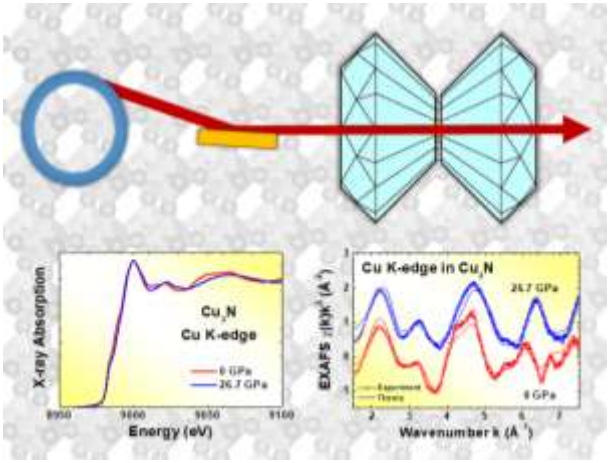

Upper panel: scheme of pressure-dependent X-ray absorption spectroscopy experiment using diamond anvil cell. Left panel: Pressure-dependence of the Cu K-edge XANES of Cu_3N. Right panel: comparison of the experimental (open circles) and calculated (solid lines) Cu K-edge EXAFS spectra $\chi(k)k^2$ of Cu_3N at 0 and 26.7 GPa.

The analysis of X-ray absorption near-edge structure (XANES) and extended X-ray absorption fine structure (EXAFS), based on theoretical full-multiple-scattering and single-scattering approaches, respectively, suggests that at all pressures the local atomic structure of Cu_3N remains close to that in cubic *Pm-3m* phase. Therefore, the transition to metal state above 5 GPa is explained by the band gap collapse due to a decrease of the unit cell volume. In particular, the lattice parameter of Cu_3N is reduced by ≈2% upon increasing pressure up to 26.7 GPa, and the structure is restored upon pressure release.

The paper was selected for Back Cover of Physica Status Solidi B special issue on Synchrotron Radiation: Progress of Data Analysis, Data-Driven Science, and Theory for Science.

Published in:

A. Kuzmin, A. Anspoks, A. Kalinko, J. Timoshenko, L. Nataf, F. Baudelet, T. Irifune, Origin of pressure-induced metallization in Cu_3N: an X-ray absorption spectroscopy study, Phys. Status Solidi B 255 (2018) 1800073:1-6. DOI: 10.1002/pssb.201800073. (IF=1.729, SNIP=0.786)

Kinetics of the electronic center annealing in Al_2O_3 crystals

V.N. Kuzovkov, E.A. Kotomin, and A.I. Popov
Institute of Solid State Physics, University of Latvia, Kengaraga Street 8, LV-1063, Riga, Latvia

α-Al_2O_3 (corundum, sapphire) is important radiation-resistant material with potential applications in fusion reactors, e.g. for components of diagnostic windows. The radiation produces in oxygen sublattice electronic defects (color centers)- vacancies with trapped one or two electrons (the F^+ and F centers, respectively) and more complex defects (e.g. dimers $\boldsymbol{F_2}$).

The experimental annealing kinetics of the primary electronic $\boldsymbol{F}$, F^+ centers and dimer $\boldsymbol{F_2}$ centers observed in Al_2O_3 produced under neutron irradiation were carefully analyzed. The developed theory takes into account the interstitial ion diffusion and recombination with immobile F-type and F_2-centers, as well as mutual sequential transformation with temperature of *three types* of experimentally observed dimer centers which differ by net charges (0, +1, +2) with respect to the host crystalline sites. The relative initial concentrations of three types of $\boldsymbol{F_2}$ electronic defects before annealing are obtained, along with energy barriers between their ground states as well as the relaxation energies.

Analysis of the kinetics of the mutual transformation of three types of dimer F_2-type centers observed under intensive neutron irradiation allows us to extract all kinetic parameters and supports the idea that these three centers differ by the charge states (neutral, single- and double-charged defects with respect to the perfect crystal).

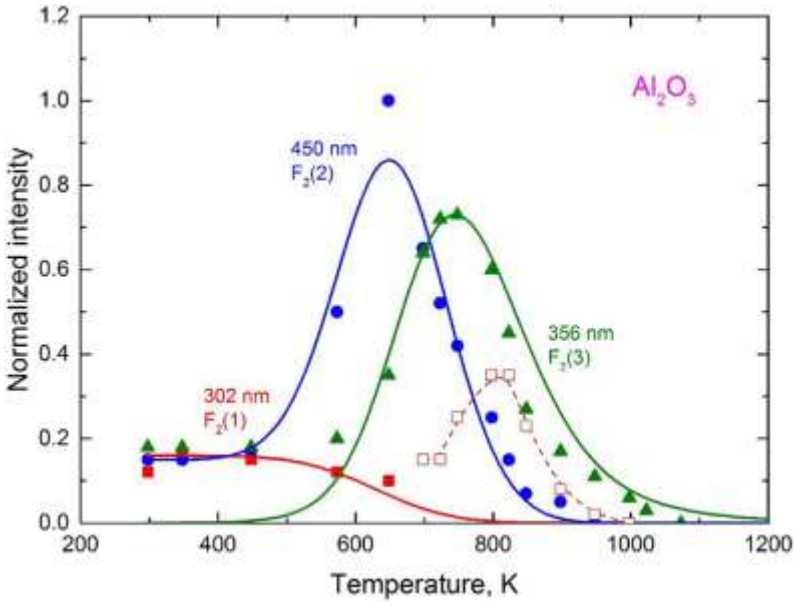

Experimental points and their theoretical analysis (full lines). Maximum of the 450 nm band intensity was normalized to unity. Background was substracted and peaks normalized.

Published in:
V.N. Kuzovkov, E.A. Kotomin, and A.I. Popov. Kinetics of the electronic center annealing in Al_2O_3 crystals. *J. Nucl. Mater.*, **502** (2018) 295-300. *DOI: 10.1016/j.jnucmat.2018.02.022 (IF=2.447, SNIP=1.380).*

Ordering of fluorite-type phases in erbium-doped oxyfluoride glass ceramics

Guna Krieke, Anatolijs Sarakovskis, Maris Springis
Institute of Solid State Physics, University of Latvia, Kengaraga Street 8, LV-1063, Riga, Latvia

For the first time nanocrystalline erbium doped glass ceramics containing rhombohedral $Ba_4Yb_3F_{17}$ and tetragonal NaF-BaF_2-YbF_3 ordered fluorite related phases were prepared from melt-quenched precursor glasses. Intense red upconversion luminescence observed under near-infrared excitation is explained by efficient cross-relaxation processes between erbium and ytterbium ions.
In BaF_2 nanocrystallites containing glass ceramics luminescence corresponding to isolated Er^{3+} sites and their clusters was detected. For the glass ceramics heat treated at lower temperature the formation of the cluster sites was dominant, whereas the heat treatment of the glass ceramics at higher temperatures increased the relative number of single Er^{3+} sites in BaF_2 nanocrystals suggesting that Er^{3+} ions act as nucleating agents during the crystallization of BaF_2.
The introduction of YbF_3 in the precursor glass promoted the formation of solid solutions with fluorite-type structure. The results of DTA, XRD as well as site-selective spectroscopy data analysis demonstrate the ordering of fluorite-type structure upon the heat treatment of the precursor glasses. Two ordered phases with rhombohedrally ($Ba_4Yb_3F_{17}$ for glass ceramics with low YbF_3 content) and tetragonally (NaF-BaF_2-YbF_3 solid solution in the glass ceramics with higher YbF_3 content) distorted fluorite structure were confirmed. The results show that the site-selective spectroscopy of rare earth ions is an essential tool to study the phase formation of the nanocrystalline structures.

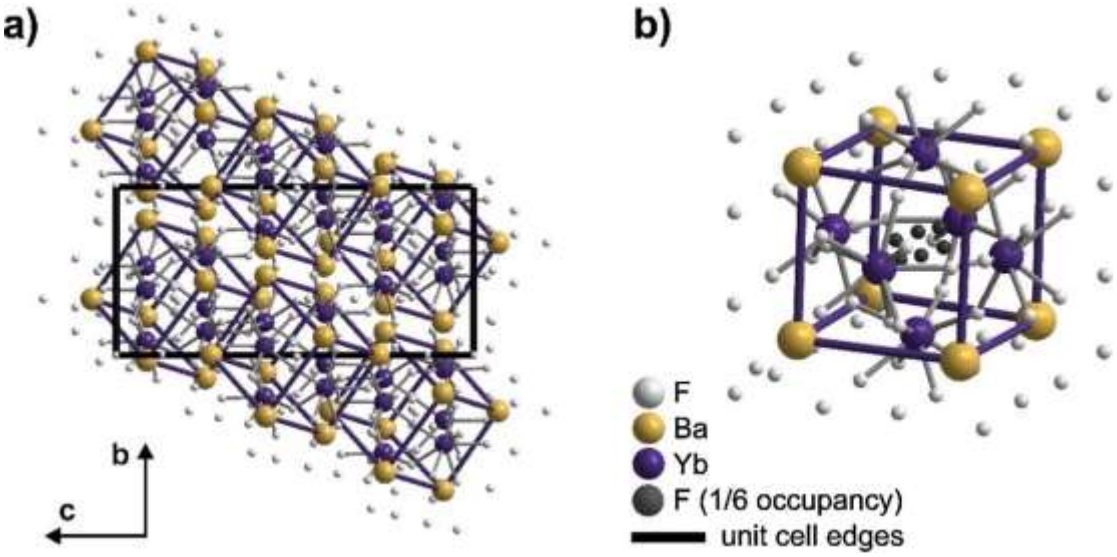

a) Crystal structure of the rhombohedral $Ba_4Yb_3F_{17}$, projection along a axis an axis and b) $Ba_8Yb_6F_{68}$ structural unit.

Published in:
Krieke, G., Sarakovskis, A., Springis, M., Ordering of fluorite-type phases in erbium-doped oxyfluoride glass ceramics (2018) Journal of the European Ceramic Society, 38 (1), pp. 235-243.

Phase transitions and upconversion luminescence in oxyfluoride glass ceramics containing $Ba_4Gd_3F_{17}$ nanocrystals

G. Krieke, A. Sarakovskis, R. Ignatans, J. Gabrusenoks
Institute of Solid State Physics, University of Latvia, Kengaraga Street 8, LV-1063, Riga, Latvia

Recently considerable attention has been devoted to investigation of rare earth doped materials for upconversion luminescence. Among others oxyfluoride glass ceramics containing barium rare earth fluoride nanocrystals are excellent candidates for applications in which transparency is required.

In this study novel transparent Er^{3+} doped oxyfluoride glass-ceramics containing $Ba_4Gd_3F_{17}$ nanocrystals were prepared by melt quenching followed by heat treatment of as-prepared glasses. The phase composition, microstructure were investigated by X-ray diffraction, scanning electron microscopy and transmission electron microscopy. The spectroscopic properties of glass ceramics were compared with single phase cubic and rhombohedral $Ba_4Gd_3F_{17}$ ceramics. The local environment of Er^{3+} and the phonon energy of both polymorphs were analyzed using luminescence and Raman spectroscopy.

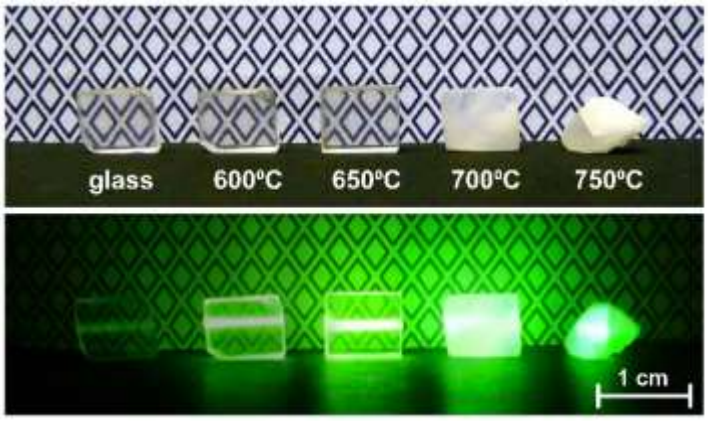

Photographs of the Er^{3+} doped glass and glass ceramics heat treated at different temperatures: upper row – as prepared, lower row – excited with 975 nm laser.

In the temperature range of 650-700°C, a phase transition from metastable cubic to rhombohedrally distorted fluorite phase in the glass ceramics was detected using Er^{3+} as a probe.

Intense upconversion luminescence resulting from energy transfer between erbium ions was observed under near-infrared excitation (975 nm). Longer characteristic decay times and splitting of the luminescence bands compared to the precursor glass indicated the incorporation of erbium ions in the crystalline phase. The intensity of the upconversion luminescence in the glass ceramics with rhombohedral $Ba_4Gd_3F_{17}$ nanocrystals was two orders of magnitude higher than in the precursor glass and at least two times higher than in the cubic phase.

In conclusion, low local symmetry of RE^{3+} (C_1) and low effective phonon energy (310 cm^{-1}) of rhombohedral $Ba_4Gd_3F_{17}$ nanocrystals make this glass ceramics a desirable host for UCL applications.

Published in:
G. Krieke, A. Sarakovskis, R. Ignatans, J. Gabrusenoks, Journal of the European Ceramic Society 37 (2017) 1713-1722, DOI: 10.1016/j.jeurceramsoc.2016.12.023 (IF=3.411, SNIP=1.776).

X-ray absorption spectroscopy of thermochromic phase transition in $CuMoO_4$

I. Jonane[a], A. Cintins[a], A. Kalinko[b], R. Chernikov[c], A. Kuzmin[a]
[a] *Institute of Solid State Physics, University of Latvia, Riga, Latvia*
[b] *Department Chemie, Naturwissenschaftliche Fakultät, Universität Paderborn, Paderborn, Germany*
[c] *DESY Photon Science, Hamburg, Germany*

Copper molybdate ($CuMoO_4$) attracts considerable interest due to its thermochromic and piezochromic properties, which originate from the first order phase transition between the γ and α phases. Based on diffraction data, the γ-to-α phase transition is described as "pseudoreconstructive" with an extensive two phase coexistence range and hysteretic behavior. A deep understanding of the structure-thermochromic property relationship in $CuMoO_4$ requires detailed information on the temperature dependence of the local atomic structure. In this work, thermochromic phase transition was studied in $CuMoO_4$ using the Cu and Mo K-edge X-ray absorption spectroscopy in the temperature range of 10–300 K.

The hysteretic behavior of transition was evidenced from the temperature dependence of the pre-edge shoulder intensity at the Mo K-edge, indicating that the transition from brownish-red γ-$CuMoO_4$ to green α-$CuMoO_4$ occurs in the temperature range of 230–280 K upon heating, whereas the α-to-γ transition occurs between 200 and 120 K upon cooling. The analysis of X-ray absorption near edge structure (XANES) was supported by ab initio full-multiple-scattering calculations.

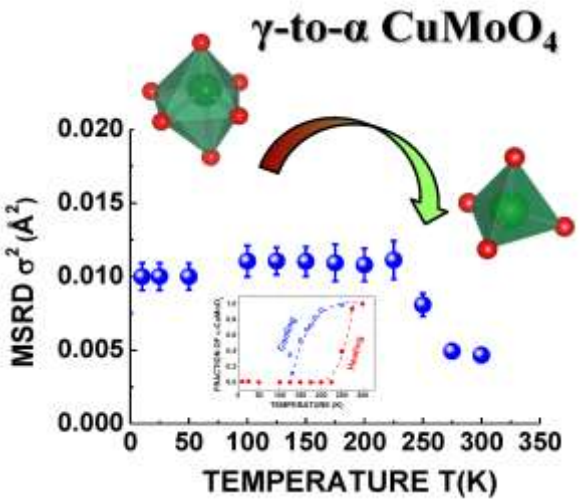

Temperature dependence of the mean-square relative displacement (MSRD) σ^2 for the four shortest Mo–O interatomic distances in $CuMoO_4$. Inset: the phase transition hysteresis obtained from the Mo K-edge XANES of $CuMoO_4$ upon heating and cooling

The temperature dependence of the radial distribution function (RDF) for the Mo–O atom pairs in the first coordination shell of molybdenum atoms reconstructed by the regularization-like method from the extended X-ray absorption fine structure (EXAFS) spectra suggests that the transition occurs gradually within the two-phase coexistence range. The local environment of molybdenum atoms transforms upon the γ-to-α phase transition from strongly distorted octahedral to less distorted tetrahedral coordination in agreement with the behavior of the pre-edge shoulder at the Mo K-edge.

Published in:

1. *I. Jonane, A. Cintins, A. Kalinko, R. Chernikov, A. Kuzmin, Probing the thermochromic phase transition in $CuMoO_4$ by EXAFS spectroscopy, Phys. Status Solidi B 255 (2018) 1800074:1-5. DOI: 10.1002/pssb.201800074. (IF=1.729, SNIP=0.786)*
2. *I. Jonane, A. Cintins, A. Kalinko, R. Chernikov, A. Kuzmin, X-ray absorption near edge spectroscopy of thermochromic phase transition in $CuMoO_4$, Low Temp. Phys. 44 (2018) 434-437. DOI: 10.1063/1.5034155. (IF=0.86, SNIP=0.522)*

Electromechanical properties of Na0.5Bi0.5TiO³-SrTiO³-PbTiO³ solid solutions

Š.Svirskas[a], M.Dunce[b], E.Birks[b], A.Sternbergs[b], J.Banys[a]
[a] *Vilnius University, Deparment of Ferroelectrics*
[b] *Institute of Solid State Physics, University of Latvia, Kengaraga Street 8, LV-1063, Riga, Latvia*

Thorough studies of electric field-induced strain are presented in $0.4Na_{1/2}Bi_{1/2}TiO_3$-(0.6-x)$SrTiO_3$-$x$$PbTiO_3$ (NBT-ST-PT) ternary solid solutions. The increase of concentration of lead x induces crossover from relaxor to ferroelectric. Strain in a relaxor state can be described by electrostrictive behaviour. The electrostrictive coefficients correspond to other well-known relaxor ferroelectrics.

The concentration region with a stable ferroelectric phase revealed that the polarization dependence of strain does not exhibit nonlinearity, although they are inherent to the electric field dependence of strain. In this case, electric field dependence of strain is described in terms of the Rayleigh law and the role of domain wall contribution is extracted.

Finally, the character of strain at the electric field-induced phase transition between the nonpolar and the ferroelectric states is studied. The data shows that in the vicinity of the electric field induced phase transition the strain vs. electric field displays electrostrictive character.

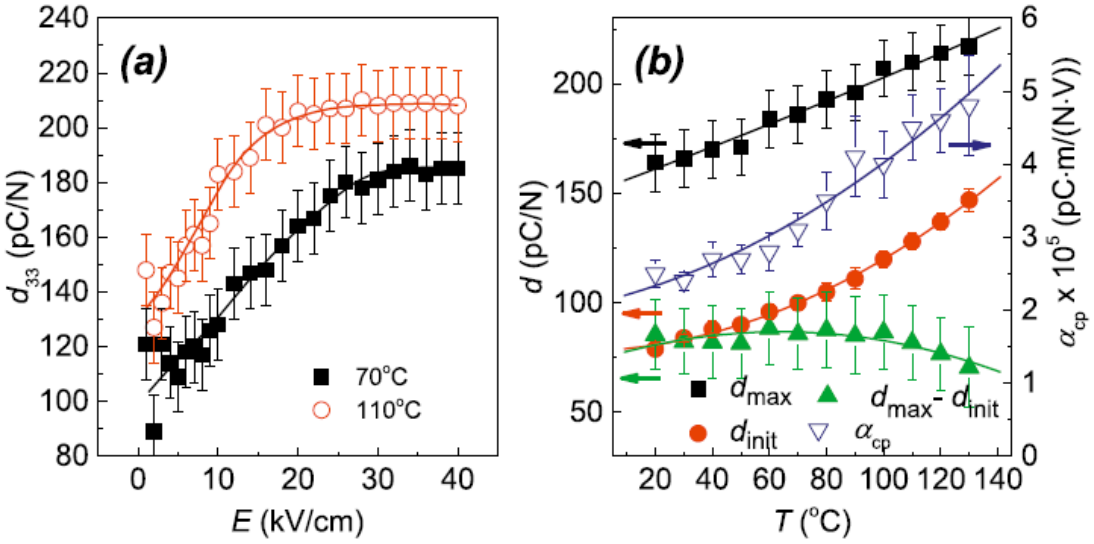

Piezoelectric coefficient as a function of the electric field amplitude $d_{33}(E_{max})$ for the composition 0.4NBT-0.4$SrTiO_3$-0.2$PbTiO_3$ at 70°C and at 110°C (a), as well as temperature dependence of the extracted values of the parameters entering in Rayleigh formula (b).

Published in:
Š.Svirskas, M.Dunce, E.Birks E., A.Sternbergs, J.Banys. Electromechanical properties of Na0.5Bi0.5TiO3-SrTiO3-PbTiO3 solid solutions. J.Phys.Chem.Sol., 114, 94 (2018).

The role of disorder on Er3+ luminescence in Na1/2Bi1/2TiO3

M.Dunce, G.Krieke, E.Birks, M.Antonova, L.Eglite, J.Grube, A.Sarakovskis

Institute of Solid State Physics, University of Latvia, Kengaraga Street 8, LV-1063, Riga, Latvia

Photoluminescence in Er-doped NBT is studied at different temperatures. Remarkable reduction of the luminescence intensity in the green spectral range is found in the poled state comparing with the depoled state. Luminescence spectra at low temperatures reveal continuous wavelength shift of some maxima belonging to the $^4S_{3/2} \rightarrow {}^4I_{15/2}$ transition depending on the excitation wavelength, which is explained by large variety of different environments around Er^{3+} related to the random distribution of Na^+ and Bi^{3+} in A-sublattice of the ABO_3 perovskite structure. Poling extends the wavelength range where shift of luminescence maxima is observed in the direction of longer excitation wavelengths. This feature can be explained by more ordered structure characteristic to the poled state comparing with the depoled one. Luminescence spectra of Er-doped $BaTiO_3$ are also measured at low temperatures, and confirm the role of Na^+ and Bi^{3+} ion disorder in the observed spectral features of Er-doped NBT.

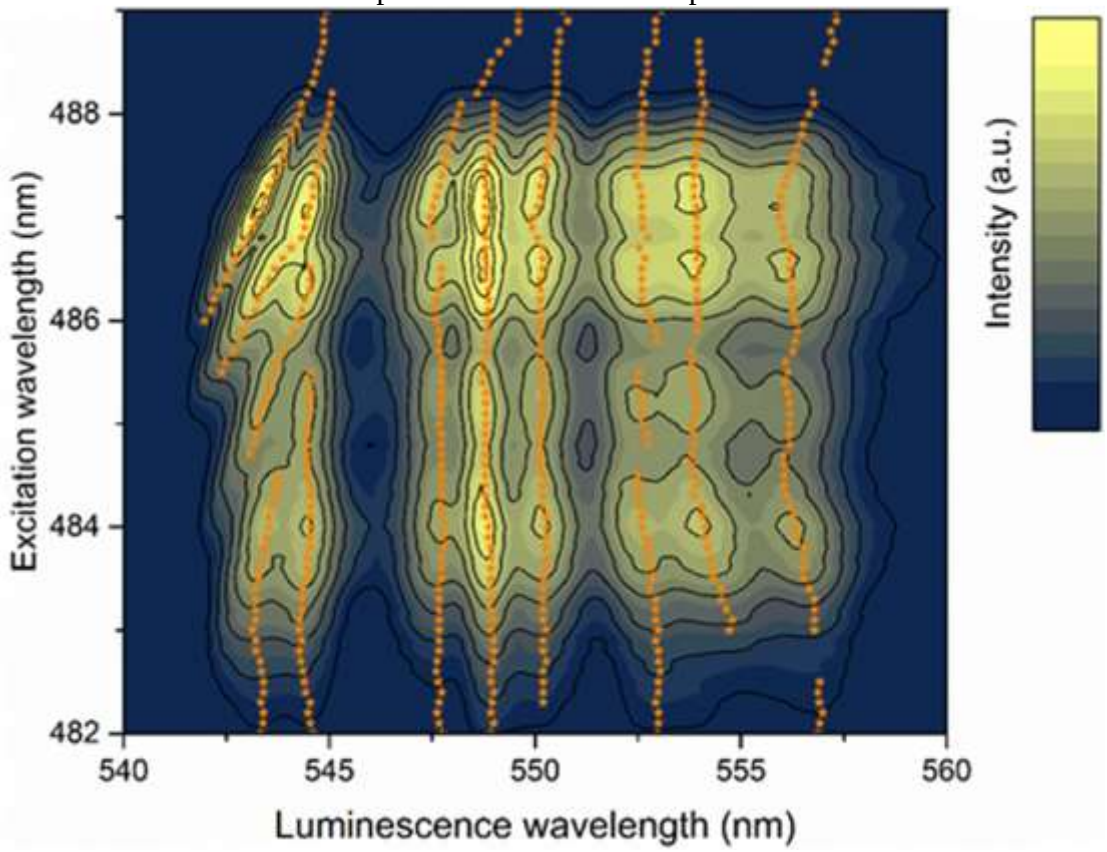

Contour plot of fixed luminescence intensity lines in dependence on emission and excitation wavelength of the Er-doped NBT composition. Shifts of particular luminescence maxima as a function of the excitation wavelength in left side are explained by variation of energetic levels, responsible for luminescence from large number of local environment of Er.

Published in:

M.Dunce, G.Krieke, E.Birks, M.Antonova, L.Eglite, J.Grube, A.Sarakovskis. The role of disorder on Er3+ luminescence in Na1/2Bi1/2TiO3. J.Alloys Compd., 762, 326 (2018)

Two-phase dielectric polar structures in 0.1NBT-0.6ST-0.3PT solid solutions.

Š.Svirskas, V.V.Shvartsman, **M.Dunce, R.Ignatans, E.Birks**, T.Ostapchuk, S.Kamba, D.C.Lupasku. J.Banys.

Institute of Solid State Physics, University of Latvia, Kengaraga Street 8, LV-1063, Riga, Latvia

Unexpected domain patterns in 0.1NBT-0.6ST-0.3PT ceramics which are responsible for a complex macroscopic response are revealed. The investigated ceramics consist of at least two different sizes of grains having different kind of polar structures. The large micron-sized grains show a clear phase transition that matches the one observed in the temperature dependence of the dielectric permittivity. On the other hand, submicron-sized grains show irregular or single domain structures which persist even above the phase transition temperature. The polar features of the smaller grains resemble polar nanoregions of relaxors. The dielectric anomaly above the transition temperature can be related to the response of these smaller grains. The contribution of larger grains to the permittivity at the phase transition is quite small and is reflected in the Terahertz properties of the sample. It indicates that the largest contribution to the dielectric anomaly comes from correlated collective motion of nano-sized polar entities in small grains.

The observed domains can be easily manipulated by external electric field. Thus it is reasonable to assume that the contribution to the macroscopic (dielectric, ferroelectric) properties is a superposition of all the different kinds of domains below T_c. In the smaller grains the correlation length changes during the phase transition resulting in the crossover from ferroelectric domain-like structures to polar nanoregions. This is evidenced by the possibility to manipulate the polarization of these small grains above T_c.

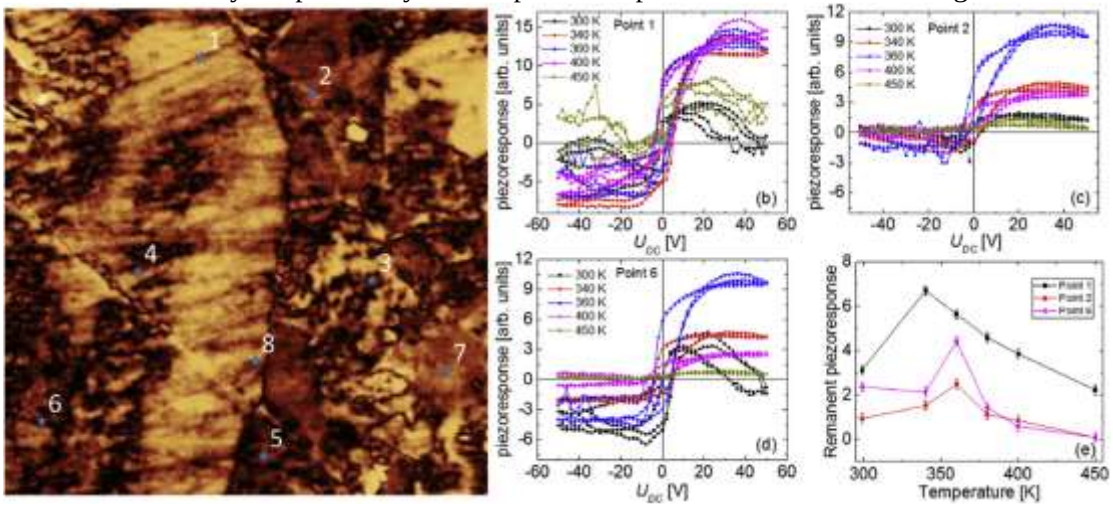

Local piezoresponse hysteresis loops measured inside a grain with irregular domain patterns of 0.1NBT-0.6$SrTiO_3$-0.3$PbTiO_3$. Measurement locations are shown in the DART PFM image (a). Panels (b)-(d) show examples of the hysteresis loops taken at different temperatures. Panel (e) shows the temperature dependences of the remanent piezoresponse for the various locations. The location 1 corresponds to a "very stable" domain, while locations 3 and 6 correspond to nanodomains.

Published in:

Š.Svirskas, V.V.Shvartsman, M.Dunce, R.Ignatans, E.Birks, T.Ostapchuk, S.Kamba, D.C.Lupasku. J.Banys. Two-phase dielectric polar structures in 0.1NBT-0.6ST-0.3PT solid solutions. Acta Mater., 153, 117 (2018)

Luminescence and energy transfer in Dy3+/Eu3+ co-doped aluminosilicate oxyfluoride glasses and glass-ceramics

M. Kemere, U. Rogulis
Institute of Solid State Physics, University of Latvia, Kengaraga Street 8, LV-1063, Riga, Latvia

Oxyfluoride glass-ceramics have been widely investigated in the last years because of their favourable properties the stability of the oxide matrix and the low phonon energy of fluoride nanocrystallites. In oxyfluoride glass-ceramics, rare-earth (RE) ions tend to segregate preferentially in the fluoride nanocrystallites by occupying the cationic positions in the nanocrystallites. When incorporated into nanocrystallites, RE ions find themselves in strictly ordered surroundings with a lower phonon energy than in the glass phase. As a result, the luminescence emission intensity and the quantum efficiency of the RE ions in the material can be improved and are similar to that in the single fluoride crystals. Among the applications in lighting devices, WLEDs, the low phonon energy of fluoride nanocrystallites is essential for upconverted luminescence processes as well, Er^{3+}, Yb^{3+} and Tm^{3+} doped materials have promise in solar cells, infrared light converters and applications in medicine.

A series of oxyfluoride SiO_2-CaF_2-Al_2O_3-CaO-Eu_2O_3-Dy_2O_3 glasses were synthesized using the melt quenching method starting from high purity raw materials in powder form. The glass-ceramics were obtained from the prepared glasses

using the heat treatment method. To introduce the CaF_2 crystalline phase into the samples, the precursor glasses were annealed isothermally at 680 ^{O}C or 750 ^{O}C for 1 h, then removed from the furnace and cooled down in air.

The glasses doped with 0.5 mol% of Dy^{3+} showed the highest emission intensity compared with the Dy^{3+}/Eu^{3+} co-doped samples and the samples doped with Dy^{3+} in higher concentrations (1 mol%). The average luminescence lifetimes of Dy^{3+} ($^4F_{9/2}/^6H_{13/2}$) decreased linearly with the addition of Eu^{3+} ions in the concentration range of 0-2 mol% Eu^{3+}. With higher Eu^{3+} concentration, luminescence lifetimes deviated from the linear correlation due to concentration quenching of the Eu^{3+} ions.

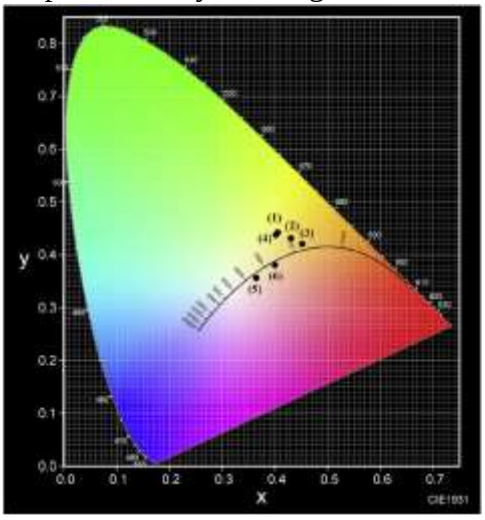

The colour coordinates of the samples under 453 nm excitation for most of the studied concentrations were close to those of white light. For 350 nm excitation, white light was achieved for the Dy^{3+} codoped samples in which the concentrations of and Eu^{3+}

ions were nearly equal.

Published in:
Kemere, M., Rogulis, U., Sperga, J., Luminescence and energy transfer in Dy3+/Eu3+ co-doped aluminosilicate oxyfluoride glasses and glass-ceramics (2018) Journal of Alloys and Compounds, 735, pp. 1253-1261.

Fast-Response Single-Nanowire Photodetector Based on ZnO/WS_2 Core/Shell Heterostructures

E. Butanovs[a], S. Vlassov[b], A. Kuzmin[a], S. Piskunov[a], J. Butikova[a], B. Polyakov[a]
[a] *Institute of Solid State Physics, University of Latvia, Riga, Latvia*
[b] *Institute of Physics, University of Tartu, Tartu, Estonia*

Nanostructured photodetectors operating from ultraviolet (UV) to terahertz frequencies have attracted much attention during the last few decades due to their appealing performance for various applications. Current developments in the field are concentrated on precisely controlling the manufacturing of nanostructured materials, modifying their properties, and developing methods for mass production. Photodetectors based on one-dimensional (1D) nanostructured materials have become one of the most attractive photoelectronic devices that can be implemented using individual or assemblies of nanostructures. A fabrication of hybrid nanostructures composed of two or more components opens new possibilities to control their properties, in particular, in photodetection capability in a broad spectral range from UV to infrared.

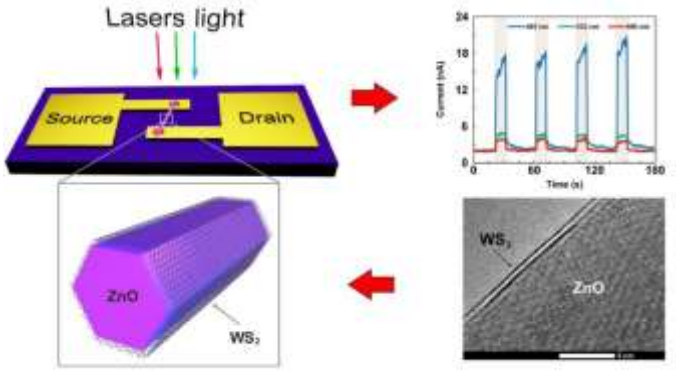

Left panels: schematics of ZnO/WS_2 core/shell nanowire-based photodetector. Right panels: on-off photoresponse measurements of ZnO/WS_2 nanowire photoresistors at 1 V bias voltage and light illumination using 0.5 W/cm^2 light intensity of 405, 532, and 660 nm wavelengths. TEM image of ZnO/WS_2 nanowire is also shown.

The surface plays an exceptionally important role in nanoscale materials, exerting a strong influence on their properties. Consequently, even a very thin coating can greatly improve the optoelectronic properties of nanostructures by modifying the light absorption and spatial distribution of charge carriers. To use these advantages, 1D/1D heterostructures of ZnO/WS_2 core/shell nanowires with a-few-layers-thick WS_2 shell were fabricated. These heterostructures were thoroughly characterized by scanning and transmission electron microscopy, X-ray diffraction, and Raman spectroscopy. Then, a single-nanowire photoresistive device was assembled by mechanically positioning ZnO/WS_2 core/shell nanowires onto gold electrodes inside a scanning electron microscope.

The results show that a few layers of WS_2 significantly enhance the photosensitivity in the short wavelength range and drastically (almost 2 orders of magnitude) improve the photoresponse time of pure ZnO nanowires. The fast response time of ZnO/WS_2 core/shell nanowire was explained by electrons and holes sinking from ZnO nanowire into WS_2 shell, which serves as a charge carrier channel in the ZnO/WS_2 heterostructure. First-principles calculations suggest that the interface layer i-WS_2, bridging ZnO nanowire surface and WS_2 shell, might play a role of energy barrier, preventing the backward diffusion of charge carriers into ZnO nanowire.

Published in:
E. Butanovs, S. Vlassov, A. Kuzmin, S. Piskunov, J. Butikova, B. Polyakov, Fast-response single-nanowire photodetector based on ZnO/WS2 core/shell heterostructures, ACS Appl. Mater. Interfaces 10 (2018) 13869-13876. DOI: 10.1021/acsami.8b02241. (IF=8.097, SNIP=1.543)

Effect of amorphous state of SiO_2 optical materials on the radiation-induced formation of intrinsic point defects

L.Skuja[a], N.Ollier[b], K.Kajihara[c], K.Smits[a]

[a]*Institute of Solid State Physics, University of Latvia, LV-1063, Riga, Latvia*
[b]*LSI, Ecole Polytechnique, University of Paris-Saclay, 91128 Palaiseau, France*
[c]*Tokyo Metropolitan University, Hachioji,Tokyo 192-0397, Japan*

High purity or synthetic silica is the toughest glassy optical material for use in radiation environments or high-power laser applications. Point defects - dangling bonds, vacancies and interstitial atoms set limits to the radiation toughness. It is different between the glassy and crystalline SiO_2, despite the similar near-range structure (corner-shared SiO_4 tetrahedra) in both states. This problem has been extensively studied, however, mostly by using irradiation modes, causing nano-scale or meso-scale locally amorphized regions in crystal. That comprises studies, which use high-energy nuclear particles or low-energy electrons, absorbed in thin layers. The behavior of the most important point defects (dangling O and Si bonds, oxygen vacancies and interstitials) in non-amorphized quartz is still not well-understood.

We performed a study of super-high purity α-quartz irradiated by 2.5 MeV electrons, that is, under conditions, which provide for vacancy-interstitial creation, but exclude the formation of amorphized particle tracks. The maximum dose (3×10^{19} e^-/cm^2) was just below the amorphization threshold of SiO_2. The optical properties were studied by luminescence techniques, and the data were compared to those for neutron-irradiated quartz and glassy SiO_2.

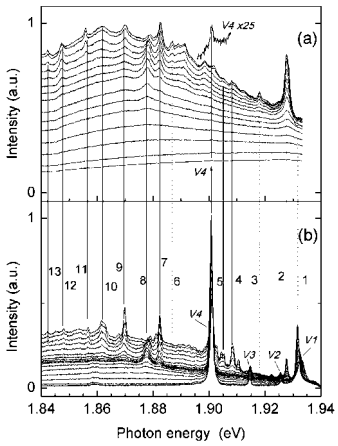

Comparison of high-resolution low-temperature (T=14K) luminescence spectra of e^- (b) and neutron- irradiated (a) α-quartz, demonstrating the emergence of highly-ordered oxygen dangling bonds in crystalline SiO_2. V1-V4 are Raman bands Excitation at $\hbar\omega$= 1.959 eV.

The results show for the first time that oxygen dangling bonds ("NBOHC"), characteristic to the glassy state, can be created in *non-amorphized* SiO_2 crystal. In comparison to the dangling O bonds created in neutron-damaged quartz, their environment is much more ordered, as illustrated (Fig) by narrowing of their site-selective luminescence lines and their higher amplitude relative to the continuum.

In contrast to the cases of neutron-irradiated α-quartz and glassy SiO_2, interstitial oxygen atoms knocked out by e^- irradiation, did not form O_2 molecules, illustrating that interstitial spaces in α-quartz are insufficiently large for their formation. They evidently form peroxy linkages (Si-O-O-Si bonds). Their optical properties are still poorly known and are a subject of our present studies.

Published in:
L. Skuja, N. Ollier, K. Kajihara, K. Smits, Creation of glass-characteristic point defects in crystalline SiO_2 by 2.5 MeV electrons and by fast neutrons, J. Non-Cryst. Solids. ***505*** *(2019) 252–259. doi:10.1016/j.jnoncrysol.2018.11.014. (IF=2.34, SNIP=1.19).*

Optical phase recovery from light intensity measurements using a single binary amplitude modulating mask

V. Karitāns, E. Nitiss, A. Tokmakovs
Institute of Solid State Physics, University of Latvia, Kengaraga Street 8, LV-1063, Riga, Latvia

In various fields of signal processing and especially optics, one often faces the phase problem, i.e., a detector can only record intensity while the information about phase is lost. Various methods have been proposed to recover the missing information about phase. In optics, during the last years methods recovering the phase from intensity measurements by modulating the light beam become increasingly popular. In this study, we investigate whether the optical phase can be recovered using a single binary amplitude modulating mask by rotating it in four different positions.

First, we carry out simulations to verify whether a single mask is sufficient for reasonable recovery. We generate a random wavefront and modulate it with a mask containing only zeros and ones. We calculate the corresponding diffraction pattern and apply a PhaseLift method to recover the phase. Simulations show perfect reconstruction of the original wavefront with small noise superimposed on it probably due to the low number of modulating masks.

We also carried out practical experiments by spin-coating polydimethylsiloxane (PDMS) on a glass substrate. Again, we applied the PhaseLift method to recover the structure of object from intensity measurements. The masks were designed using the optical lithography. Size of the masks was 64 x 64 pixels one pixel being equal to 80 μm. The wavefront measured with the Shack-Hartmann aberrometry was selected as the reference wavefront. Similarity, between the reconstructed wavefront and the reference wavefront can also be noted.

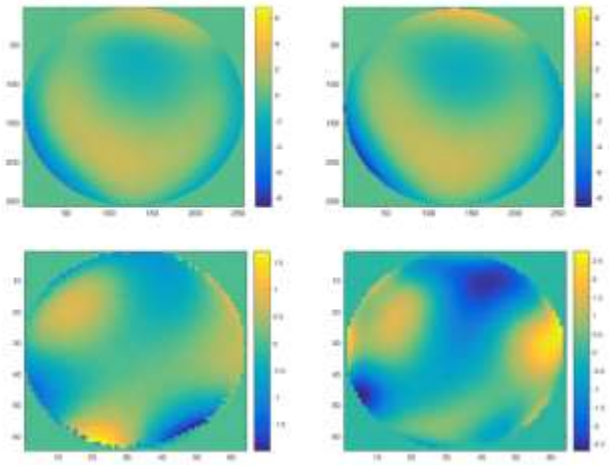

Augšējā rinda – simulācijas. Pa kreisi – simulētā viļņu fronte; pa labi – rekonstruētā viļņu fronte. Apakšējā rinda – praktiski mērījumi. Pa kreisi – atskaites viļņu fronte; pa labi – rekonstruētā viļņu fronte.

The algorithm PhaseLift recovering the phase from intensity measurements seems to perform well even in the case of a very few modulating masks. The biggest problem with the algorithm PhaseLift is time-consuming limiting its applicability for real-time wavefront correction. While the data on performance of PhaseLift in presence of noise is still to be estimated it also seems that PhaseLift can successfully recover the phase in low signal-to-noise ratio (SNR).

Published in:
V. Karitans, E. Nitiss, A. Tokmakovs, and K. Pudzs.
Optical phase retrieval using four rotated versions of a single binary mask – simulation results.
Proc. SPIE, 2018, 10694, 106940C (pp. 1-7).

Fast-Response Single-Nanowire Photodetector Based on ZnO/WS_2 Core/Shell Heterostructures

Edgars Butanovs[1], Sergei Vlassov[2], Alexei Kuzmin[1], Sergei Piskunov[1], Jelena Butikova[1], and Boris Polyakov[1]

[1]*Institute of Solid State Physics, University of Latvia, Kengaraga Str. 8, LV-1063, Riga, Latvia*

[2]*Institute of Physics, University of Tartu, W. Ostwaldi 1, 50411 Tartu, Estonia*

The surface plays an exceptionally important role in nanoscale materials, exerting a strong influence on their properties. Consequently, even a very thin coating can greatly improve the optoelectronic properties of nanostructures by modifying the light absorption and spatial distribution of charge carriers. To use these advantages, 1D/1D heterostructures of ZnO/WS_2 core/shell nanowires with a-fewlayers-thick WS_2 shell were fabricated. These heterostructures were thoroughly characterized by scanning and transmission electron microscopy, X-ray diffraction, and Raman spectroscopy. Then, a single-nanowire photoresistive device was assembled by mechanically positioning ZnO/WS_2 core/shell nanowires onto gold electrodes inside a scanning electron microscope.

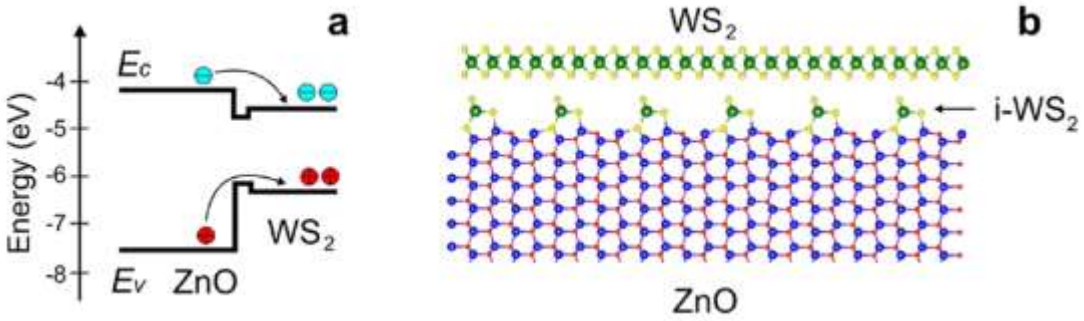

Simplified band diagram of the ZnO/WS2 core−shell NW (a). Atomic structure of ZnO/WS2 interface (b).

An effective photodetector based on ZnO/WS_2 core/shell nanowire is demonstrated in this work. The photodetector responds to illumination at the wavelengths of 660 nm, 532 nm, and 405 nm. The ZnO/WS_2 core/shell nanowire-based device shows a clear advantage over pure ZnO nanowire-based photodetector in terms of both higher responsivity (4.6-fold) and faster operation (90-fold) for 405 nm illumination. The photodetector band diagram was supported by the first principles calculations, suggesting that the interface layer i-WS_2, bridging ZnO nanowire surface, and WS_2 shell, might play an important role in preventing backward diffusion of charge carriers into the ZnO nanowire, whereas WS_2 shell serves as a charge carrier channel in the ZnO/WS2 heterostructure. The obtained results clearly show the potential of combining layeread 2D TMDs materials with semiconducting nanowires to create novel core/shell heterostructures with advanced optoelectronic properties.

Published in:

E. Butanovs, S. Vlassov, A. Kuzmin, S. Piskunov, J. Butikova, and B. Polyakov. Fast-response single-nanowire photodetector based on ZnO/WS2 core/shell heterostructures. ACS Appl. Mater. Interfaces, 2018, 10, pp. 13869–13876. DOI: 10.1021/acsami.8b02241 SNIP(2017)=1.543, IF(2017)=8.097

Energy
Domain: Energy

XAFS Synchrotron radiation studies of construction nuclear materials

J. Purāns, A. Anspoks, A. Cintiņš, I. Jonāne, A. Kuzmins, J. Timošenko
Institute of Solid State Physics, University of Latvia, Kengaraga Street 8, LV-1063, Riga, Latvia

https://www.euro-fusion.org

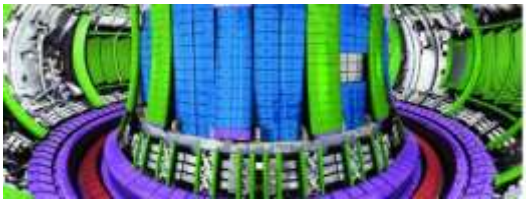

One of the main challenges for the next generation of nuclear fusion reactors is to improve the resistance of construction materials towards radiation- and heat-induced damage. This year we have completed HORIZON 2020 EUROFUSION project “When and how ODS nanoparticles are formed?” By using the world’s leading synchrotron radiation big facilities, we investigated the local structure of oxide dispersion-strengthened (ODS) ferritic steels and investigated the formation mechanisms of the nanoparticles within the structural materials for the next generation of fusion reactors. These materials are promising for high-temperature applications, allowing one to increase the reactor working temperature above 650°C.

In this project we have carried out a series of X-ray absorption spectroscopy experiments, to obtain experimental evidences about the formation of nanoparticles within ODS steels during different manufacturing stages, to optimize the manufacturing process and to validate existing theoretical models. By using world’s leading synchrotron radiation big facilities (Figure 1), we have developed a **new methodology** for the investigations of nanoparticles formation mechanisms with the ODS steels. In a series of X-ray absorption experiments we have **discovered the formation mechanisms** of oxide nanoparticles, and investigated, how are formed and what happens with the oxide nanoparticles during different stages of steel production. It allowed significant improvements in the steel manufacturing process (Figure 2).

Figure 1. ELETTRA - world's leading synchrotron radiation big facility and experimental beamlines (Italy, Trieste).

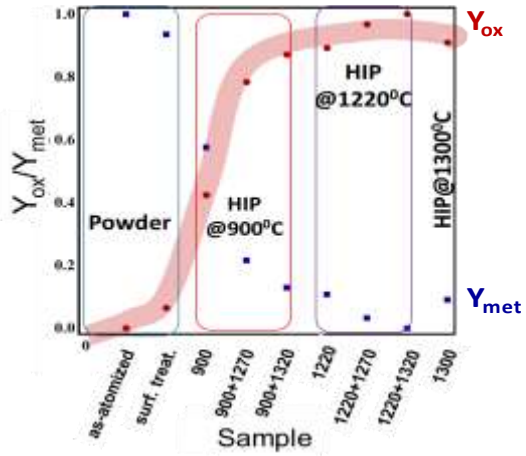

Figure 2. Linear combination analysis of the XANES spectra. Experimental evidences about the formation of nanoparticles within ODS steels during different manufacturing stages treatments: high pressure (HIP) and high temperature.

Published in:

1. J. Timoshenko, A. Anspoks, A. Cintins, A. Kuzmin, J. Purans, A.I. Frenkel, Neural network approach for characterizing structural transformations by x-ray absorption fine structure spectroscopy, Phys. Rev. Lett. 120 (2018) 225502:1-6

2. N. Ordás, E. Gil, A. Cintins, V. de Castro, T. Leguey, I. Iturriza, J. Purans, A. Anspoks, A. Kuzmin, A. Kalinko, The role of yttrium and titanium during the development of ODS ferritic steels obtained through the STARS route: TEM and XAS study, J. Nucl. Mater. 504 (2018) 8-22.

3. D. Pazos, A. Cintins, V. De Castro, P. Fernández, J. Hoffmann, W. García-Vargas, T. Leguey, J. Purans, A. Anspoks, A. Kuzmin, I. Iturriza, N. Ordás, ODS ferritic steels obtained from gas atomized powders through the STARS processing route: Reactive synthesis as an alternative to mechanical alloying, Nucl. Mater. Energy 17 (2018) 1-8.

4. T. Gräning, M. Rieth, A. Möslang, A. Kuzmin, A. Anspoks, J. Timoshenko, A. Cintins, J. Purans, Investigation of precipitate in an austenitic ODS steel containing a carbon-rich process control agent, Nucl. Mater. Energy 15 (2018) 237-243.

5. I. Jonane, A. Anspoks, A. Kuzmin, Advanced approach to the local structure reconstruction and theory validation on the example of the W L3-edge extended X-ray absorption fine structure of tungsten, Modelling Simul. Mater. Sci. Eng. 26 (2018) 025004 (11 pp).

Surface termination effects on the oxygen reduction reaction rate at fuel cell cathodes

Yu. A. Mastrikov[1], R. Merkle[2], E.A. Kotomin[1], M.M. Kuklja[3], and J. Maier[3]
[1]*Institute of Solid State Physics, University of Latvia, Kengaraga Str. 8, LV-1063, Riga, Latvia*
[2]*Max Planck Institute for Solid State Research, Stuttgart, Germany*
[3]*Materials Science and Engineering Department, University of Maryland, College Park, Maryland, USA*

Solid oxide fuel cells (SOFCs) continue to attract great attention as a promising source of ecologically clean and efficient electricity generation. The key factor, largely determining the SOFC performance, is the oxygen reduction reaction (ORR) rate at the surface with further oxygen incorporation into the cathode. $La_{1-x}Sr_xMnO_3$ (LSM) was one of the first ABO_3-type perovskites employed as a SOFC cathode material, which is still used in the form of porous composites with the respective electrolyte material, to increase the average ionic conductivity.

The results of first principles calculations of oxygen vacancy and oxygen adsorbate concentrations are analyzed and compared for the polar (La,Sr)O and MnO_2 (001) terminations of (La,Sr)MnO_3 fuel cell cathode materials. Both quantities strongly depend on the average Mn oxidation state (La/Sr ratio). In thin symmetrical slabs, the cation nonstoichiometry also plays an important role by modifying the average Mn oxidation state. The surface oxygen vacancy concentration for the (La,Sr)O termination is more than 5 orders of magnitude smaller when compared to the MnO_2 termination. The vacancy and adsorbed oxygen migration energies as well as the dissociation barriers of adsorbed molecular oxygen species are determined. The encounter of adsorbed atomic oxygen and surface oxygen vacancy is identified as the rate determining step of the oxygen incorporation reaction. Since the increase of atomic and molecular oxygen adsorbate concentration is limited by the typical saturation level in the range of 20% for charged adsorbates, the overall oxygen incorporation rate is predicted to be significantly smaller for the (La,Sr)O termination.

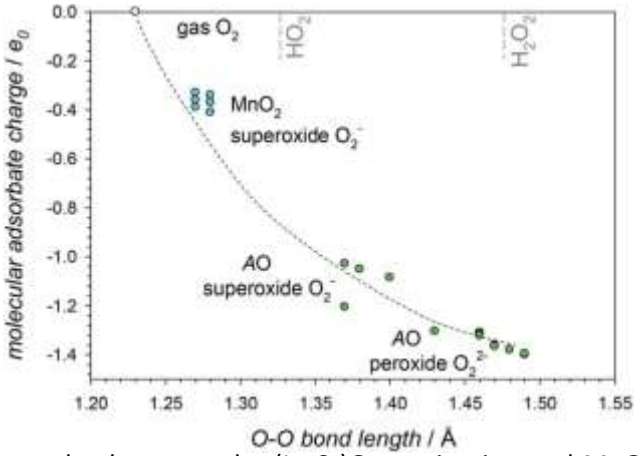

Charge of molecular oxygen adsorbates on the (La,Sr)O termination and MnO_2 termination *versus* O-O bond length. This plot allows for a distinction of superoxide vs. peroxide species.

Published in:
Yu.A. Mastrikov, R. Merkle, E.A. Kotomin, M.M. Kuklja, and J. Maier.
Surface termination effects on the oxygen reduction reaction rate at fuel cell cathodes.
J. Mater. Chem. A, 6 (2018) 11929–11940, DOI: 10.1039/c8ta02058b (IF=9.931, SNIP=1.550).

Efficiency of gyrotrons with a tapered magnetic field in the regime of soft self-excitation

O. Dumbrajs[1] and G.S. Nusinovich[2]

[1]*Institute of Solid State Physics, University of Latvia, Kengaraga Str. 8, LV-1063, Riga, Latvia*
[2]*Institute for Research in Electronics and Applied Physics, University of Maryland, College Park, Maryland 20742-3511, USA*

Gyrotrons are known as the efficient sources of millimeter-wave and sub-THz radiation capable of delivering high power in the long-pulse and continuous-wave regimes. The highest efficiency, however, is typically realized in the regime of hard self-excitation where oscillations start to grow only when their initial amplitude exceeds a certain critical level. Therefore, achieving this optimal point in the parameter space requires a special manipulation of gyrotron parameters, a so-called start-up scenario.

The gyrotron operation can be facilitated by optimizing some parameters in such a way that the maximum efficiency becomes realizable in the regime of soft self-excitation where oscillations can start to grow from the noise induced by beam electrons. One possibility to do this is to use the tapering of the external magnetic field produced by an additional small solenoid. In the present study, we consider the role of an additional small external magnetic field with parabolic tapering along the device axis, which can be produced by a small solenoid. The effect of this additional field on the efficiency and the boundaries between the regions of soft and hard self-excitation is analyzed. Our study demonstrated that small, simple additional solenoids can be used in high-power gyrotrons for improving the device efficiency in the regimes of soft and hard selfexcitation.

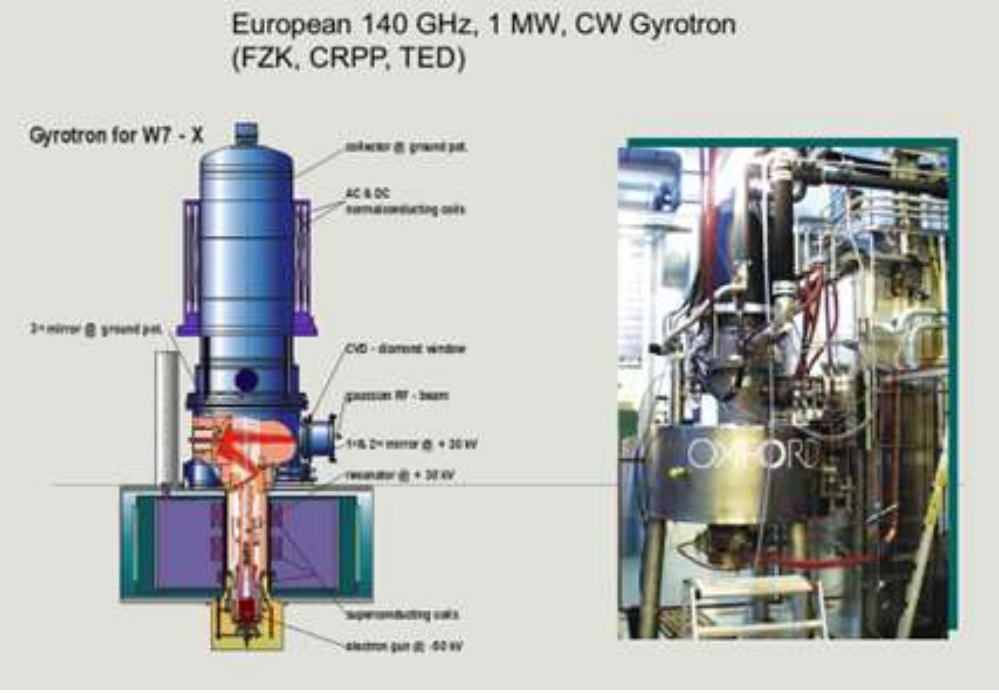

Published in:
O. Dumbrajs and G.S. Nusinovich. Efficiency of gyrotrons with a tapered magnetic field in the regime of soft self-excitation. Phys. Plasmas, 25 (2018) 013121. DOI: 10.1063/1.5019974 *(IF=1.941, SNIP=0.682).*

Synthesis and thermoelectric properties of 2- and 2,8-substituted tetrathiotetracenes

Mary Robert Garrett,[a] María Jesús Durán-Peña,[a] William Lewis,[b] Kaspars Pudzs,[c] Jānis Užulis,[c] Igors Mihailovs,[c] Björk Tyril,[a] Jonathan Shine,[a] Emily F. Smith,[d] Martins Rutkis*[c] and Simon Woodward*[a]

[a] *GSK Carbon Neutral Laboratories for Sustainable Chemistry, Jubilee Campus, University of Nottingham, Nottingham NG7 2TU, UK.*

[b] *School of Chemistry, University Park Campus, University of Nottingham, Nottingham NG7 2RD, UK*

[c] *Institute for Solid State Physics, University of Latvia, 8 Kengaraga Street, LV-1063 Riga, Latvia.*

[d] *Nanoscale and Microscale Research Centre (nmRC), School of Chemistry, University Park Campus, University of Nottingham, Nottingham NG7 2RD, UK*

E-mail: simon.woodward@nottingham.ac.uk, martins.rutkis@cfi.lu.lv

Organic thermoelectric (OTE) materials offer new opportunities for sustainable waste heat recovery, personalised power (via body heat use) and microcooling (via the Peltier effect). Recently, radical cation salts of electron-rich acene tetrathiotetracenes (TTTs) emerged as a new class of materials for OTE device preparation. Such TTT cores are highly suited to derivatisation (via position 1-4 or 7-10 functionalisation). Such derivitisation is expected to strongly affect the thermoelectric properties of the conducting states formed upon oxidation of the TTT core potentially leading to improved or tunable OTE performance. Reaction of elemental sulfur with 2-R^1 and 2,8-R^1,R^2-substituted tetracenes (**2**) in refluxing DMF affords 5,6,11,12 tetrathiotetracenes (**1**) in good yields (74-99%) for a range of substituents. The reaction rate is limited only by the solubility of the tetracene (**2**); **2g-h** being both the least soluble and slowest reacting. At partial conversion recovered single crystalline **2g** led to its X-ray structure determination. Vacuum deposited thin films from **1** (of initial 88-99% purity) show final electrical conductivities, $\sigma_{(in\ plane)}$ from 1.40 × 10^{-5} S cm^{-1} (**1g**) to 3.74 × 10^{-4} S cm^{-1} (**1b**) for the resultant near pristine films; while **1d** proved too involatile to be effectively sublimed under these conditions. In comparison, initially 95% pure TTT (**1a**) based films show $\sigma_{(in\ plane)}$ = 4.33 × 10^{-5} S cm^{-1}. The purities of **1a-h** are highly upgraded during sublimation. Well defined micro-crystallites showing blade, needle or mossy like habits are observed in the films. The Seebeck coefficients (S_b) of the prepared **1** range from 374 (**1c**) to 900 (**1f**) μV K^{-1} (vs. 855 μV K^{-1} for identically prepared 95% pure TTT, **1a**). Doping of films of **1f** (R^1 = Me, R^2 = *i*Pr) with iodine produces optimal p-type behaviour: $\sigma_{(in\text{-}plane)}$ = 7.00 × 10^{-2} S cm^{-1}, S_b = 175 μV K^{-1}. The latter's

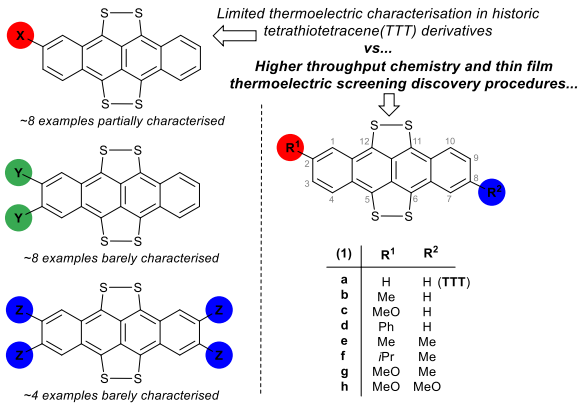

Known and new substituted tetrathiotetracenes (TTT is reserved for the parent **1a**; X-Z = alkyl derivatives, ether or amine derivatives, carbonyl derivatives, halide, CF_3, thiopyridyl).

Power Factor (*PF*) at 0.33 μW m^{-1} K^{-2} is more than 500-times that of the equivalent I_2-doped TTT films (**1a**, $R^1 = R^2 = H$), previously regarded as the optimal material for thin film thermoelectric devices using acene radical cation motifs.

Published in:
M.R.Garrett, M.J.Durán-Peña, W.Lewis, K.Pudzs, J.Užulis, I.Mihailovs, B.Tyril, J.Shine, E.F.Smith, M.Rutkis S.Woodward, Synthesis and thermoelectric properties of 2- and 2,8-substituted tetrathiotetracenes. Journal of Materials Chemistry C, 6(13) (2018) pp 3403–3409. DOI:10.1039/C8TC00073E (IF= 5.976, SNIP= 1.3)

Electrophoretically deposited α-Fe_2O_3 and TiO_2 composite anchored on rGO with excellent cycle performance as anode for lithium ion batteries

K.Kaprans, J.Mateuss, A.Dorondo, G.Bajars, G.Kucinskis, P.Lesnicenoks, J.Kleperis

Institute of Solid State Physics, University of Latvia, Kengaraga Street 8, LV-1063, Riga, Latvia

Developing devices and related materials for producing and storing electricity is a key issue to meet the increasing energy demand. Modern electronic devices require high-performance and high- energy batteries, from which Lithium-ion battery (LIB) has attracted much interest. Great efforts have been devoted to develop different types of LIB electrode materials with high reversible capacity, long cycle life and low cost.

Recently discovered graphene as a single layer of graphite possesses many excellent properties, such as good chemical stability, high quantum Hall effect, and extraordinary electronic transport properties. Besides, as a highly conducting form of carbon, graphene provides a perfect substrate to host active nanomaterials for energy applications. Separately hematite α-Fe2O3 and TiO2 are known as anode materials in LIB, but low electronic conductivity and relatively low theoretic capacity limit their application. However, there are no reports about α-Fe2O3/TiO2/graphene oxide composites as anode for LIBs prepared by electrophoretic deposition.

Two nanostructured oxides, α-Fe2O3 and TiO2 with a particle diameters 50 nm and 21 nm, were mixed with graphene oxide (GO). Composite thin films on a stainless steel substrate were obtained by electrophoretic deposition (EPD) procedure from water suspensions: α-Fe2O3/GO, TiO2/GO and α-Fe2O3/TiO2/GO. Subsequently reduction of as-prepared thin films was performed. Thicknesses of acquired films were evaluated in the range of 2–6 μm. Structure and morphology were investigated as well as electrochemical properties of all samples were studied.

The results revealed that α-Fe2O3/TiO2/rGO (in this article denoted as FTGO) exhibited the specific discharge capacity of 790 mAh·g−1 after 150 cycles at the current density 100 mA·g−1. The improved electrochemical properties were obtained due to rGO uniform dispersion within

inter-space of α-Fe2O3 and TiO2 as well as synergic effect between both metal and graphene oxides. Additionally, rGO not only has excellent electron conductivity, but also can alleviate the solid-electrolyte interphase film formation. Prepared composite exhibit excellent cycle performance, coulombic efficiency (66%) and rate capability. Therefore, FTGO ternary structure material has perspective application as lithium ion battery anode in comparison with a α-Fe2O3/rGO and TiO2/rGO composites. The results showed obtained composite is a promising anode material for high energy and long cycle life lithium ion batteries.

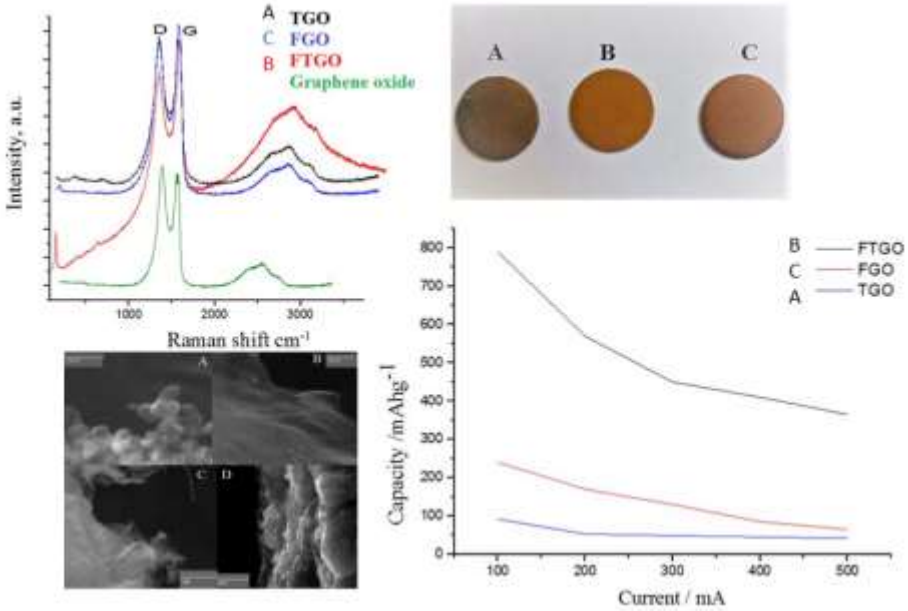

Photographs of (A) – TGO, (B)– FTGO, (C) – FGO composite electrodes, their Raman spectra and discharge rate performance.

Published in:
K.Kaprans, J.Mateuss, A.Dorondo, G.Bajars, G.Kucinskis, P.Lesnicenoks, J.Kleperis, (2018) Electrophoretically deposited α-Fe2O3 and TiO2 composite anchored on rGO with excellent cycle performance as anode for lithium ion batteries. Solid State Ionics, Volume 319, June 2018, Pages 1-6.

Comparison of LIBS results on ITER-relevant samples obtained by nanosecond and picosecond lasers

P. Paris[a], J. Butikova[b], M. Laan[a], A. Hakola[c], I. Jõgi[a], J. Likonen[c], E. Grigore[d], C. Ruset[d]

[a] *Institute of Physics, University of Tartu, Tartu 50411, Estonia*
[b] *Institute of Solid State Physics, University of Latvia, Riga LV-1063, Latvia*
[c] *VTT Technical Research Centre of Finland Ltd., 02044 VTT, Finland*
[d] *National Institute for Lasers, Plasma and Radiation Physics, Bucharest 077125, Romania*

The ITER strategy foresees applying laser induced breakdown spectroscopy (LIBS) for quantitative in situ diagnostics of fuel retention in the first walls during maintenance breaks. Quantitative information could be obtained by calibration-free LIBS, where the elemental composition of a sample is determined on the basis of the accurate knowledge of the electron temperature and the electron density. To this end, reliable detection of spectral lines of hydrogen isotopes as well as those of the host material is required.

The aim of the present study is to compare the effect of different pulse durations on LIBS results of ITER-relevant samples. Other experimental conditions, e.g. pressure and fluence, were selected to show the most clear the effect of pulse duration. The study is a necessary groundwork for following studies at atmospheric pressure relevant for actual diagnostics conditions.

LIBS spectra produced by lasers of 0.15 and 8 ns pulse durations were recorded. Experiments with ITER-relevant samples were carried out at low values of laser fluence, which allowed a reliable design of depth profiles of deuterium and tungsten. The main factor limiting the accuracy of curve-fitting of deuterium line was the high-intensity hydrogen signal.

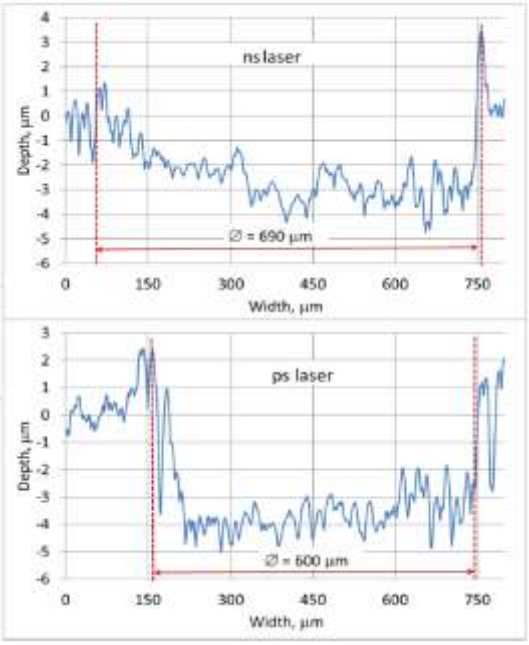

Profiles of craters formed by 30 pulses of nanosecond and picosecond lasers

Although comparatively low value of the S/N ratio has been observed for the ps laser in comparison to ns pulse width, in the case of ps laser, almost the same intensity of α-lines of hydrogen isotopes was achieved at two times lower values of laser fluence, and Intensities of W lines were less influenced by self-absorption. The latter is important considering the applications of calibration-free LIBS.

Published in:
Paris P., Butikova J., Laan M., Hakola A., Jõgi I., Likonen J., Grigore E., Ruset C.: Comparison of LIBS results on ITER-relevant samples obtained by nanosecond and picosecond lasers, Nuclear Materials and Energy, 18, pp. 1-5, 2018, DOI: https://doi.org/10.1016/j.nme.2018.11.018 (SNIP=1.351).

Ab initio modelling of the initial stages of the ODS particle formation process

Yuri A. Mastrikov[a], Maksim N. Sokolov[a], Sascha Koch[b], Yuri F. Zhukovskii[a], Aleksejs Gopejenko[a], Pavel V. Vladimirov[b], Vladimir A. Borodin[c], Eugene A. Kotomin[a], Anton Möslang[b]

[a] Institute of Solid State Physics, University of Latvia, Riga, Latvia
[b] Institute for Applied Materials, Karlsruhe Institute of Technology, Germany
[c] Kurchatov Institute, Moscow, Russia

Oxide-Dispersion Strengthened (ODS) steels with Y_2O_3 nanoparticles are promising structural materials for fusion and future fusion reactors. A large number of experimental as well as theoretical studies provided valuable information on the ODS particle formation process. However, some important details of this process still remain unexplained.

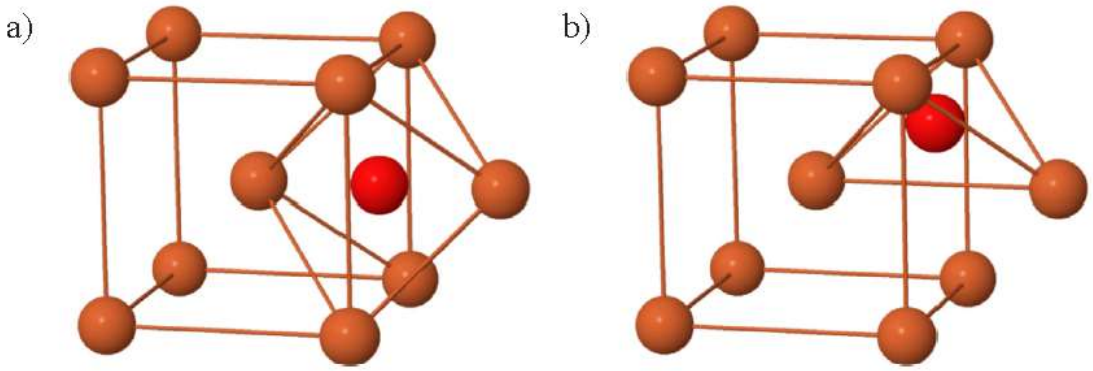

Oxygen in the bcc Fe lattice at interstitial octahedral 6b a) and tetrahedral 12d b) positions.

Our calculations have confirmed the applicability of the DFT method, as implemented in the computer code VASP, for defect calculations in ODS steels. The following particular conclusions can be drawn: vacancies precipitate, creating stable clusters in the bcc Fe lattice. Y solute atoms can be stabilized in the host matrix by vacancies. Y solute migration occurs in multiple steps by the vacancy mechanism. Clusters with 2 and 1.5 vacancies per Y solute atom provide a basis for creation Y-O bixbyite-type bonds. These results are supposed to be used at the next step of the kinetic Monte Carlo simulations of nanoparticle growth.

Published in:
Yu.A. Mastrikov, M.N. Sokolov, S. Koch, Yu.F. Zhukovskii, A. Gopejenko, P.V. Vladimirov, V.A. Borodin, E.A. Kotomin, and A. Möslang. Ab initio modelling of the initial stages of the ODS particle formation process. Nucl. Instrum. Methods Phys. Res. B, 2018, 435, pp. 70–73. DOI: 10.1016/j.nimb.2018.01.022 SNIP(2017)=1.020, IF(2017)=1.323

Ab Initio Calculations on the Electronic Structure and Photocatalytic Properties of Two-Dimensional WS_2 (0001) Nanolayers of Varying Thickness

Dmitry Bocharov[1], Sergei Piskunov[1], Yuri F. Zhukovskii[1], and Robert A. Evarestov[2]
[1]*Institute of Solid State Physics, University of Latvia, Kengaraga Str. 8, LV-1063, Riga, Latvia*
[2]*St. Petersburg State University 7/9 Universitetskaya nab., 199034 St. Petersburg, Russia*

The splitting of H_2O molecules on semiconducting electrodes under the irradiation of solar light is a clean and renewable way for the generation of hydrogen fuel. Efficiency of photocatalysis in the case of a defectless electrode depends on the relative position of the edges of the bandgap (the top of the valence band and the bottom of the conduction band), which should be properly aligned relatively to the oxidation and
reduction potentials separated by 1.23 eV.

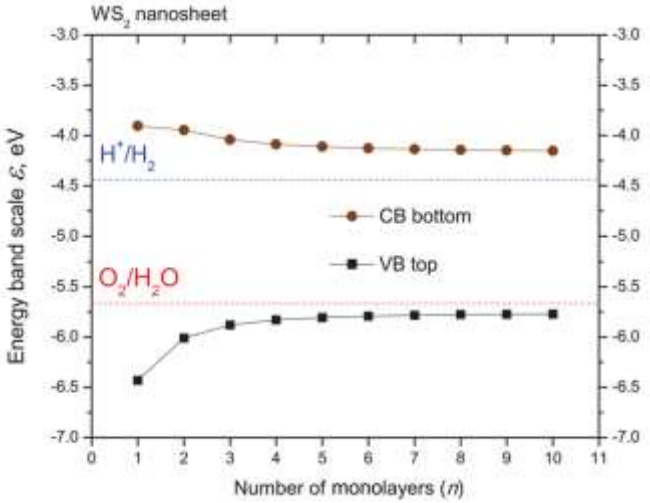

Dependence of calculated WS_2 band gap on nanosheet thickness and alignment of CB bottom and VB top edges with respect to O_2/H_2O and H^+/H_2 redox potentials.

In the current study, we have performed hybrid DFT-LCAO calculations of WS_2 nanosheets possessing stable hexagonal phase with thickness between 1 and 40 monolayers using hybrid exchange-correlation functional HSE06 adopted for this purpose. Defectless pristine WS_2 nanosheets have been found to be suitable for photocatalytic applications since widths of their band gaps correspond to the range of visible light between the red and violet edges (1.5 eV < gap < 2.7 eV) while the top of the valence band and the bottom of the conduction band are properly aligned relative to the oxidation and reduction potentials. We found that the band gap of nanolayers decreases with growing the number of monolayers in layered WS_2 2D structure. The highest solar energy conversion efficiency (15–18%) usually achieved for the gap of 2.0–2.2 eV (yellow range of the visible spectrum) has been found for the 2-monolayers thick stoichiometric WS_2 (0001) nanosheet. WS_2 nanolayers as prospective material for photocatalysis demand no doping or formation of vacancies as in the case of nanostructures of transition metal oxides. Quite the contrary, presence of these defects can worsen photocatalytic suitability of WS_2 nanolayers.

Published in:
D. Bocharov, S. Piskunov, Yu.F. Zhukovskii, and R.A. Evarestov. Ab Initio calculations on the electronic structure and photocatalytic properties of two-dimensional WS_2 (0001) nanolayers of varying thickness. Phys. Status Solidi RRL, 2018, 12, 1800253 (pp. 1-6). DOI: 10.1002/pssr.201800253 SNIP(2017)=1.017, IF(2017)=3.721

Publications in Web of Science and Scopus databases

1. G.S. Nusinovich and **O. Dumbrajs**.
   Possible gyrotron operation in the "no start current" zone caused by the axial dependence of the phase of the resonator field.
   Phys. Plasmas, 2018, **25**, 093108 (pp. 1-7).
   DOI: 10.1063/1.5045317
   SNIP(2017)=0.682, IF(2017)=1.941

2. R.I. Eglitis and **A.I. Popov**.
   Ab initio calculations of $YAlO_3$ and ABO_3 perovskite (001), (011) and (111) surfaces, interfaces and defects.
   In: *Proceedings of Xth International Scientific and Practical Conference "Electronics and Information Technologies" (ELIT-2018)*, pp. B-1 - B-4.
   DOI: 10.30970/elit2018.B01

3. A. Luchechko, Ya. Zhydachevskyy, D. Sugak, O. Kravets, N. Martynyuk, **A.I. Popov**, S. Ubizskii, and A. Suchocki.
   Luminescence properties and decay kinetics of Mn^{2+} and Eu^{3+} co-dopant ions in $MgGa_2O_4$ ceramics.
   Latv. J. Phys. Tech. Sci., 2018, **55**, n6, pp. 43-51.
   DOI: 10.2478/lpts-2018-0043
   SNIP(2017)=0.653

4. A.B. Usseinov, Yu.F. Zhukovskii, **E.A. Kotomin**, A.T. Akilbekov, M.V. Zdorovets, G.M. Baubekova, and Zh.T. Karipbayev.
   Transition levels of acceptor impurities in ZnO crystals by DFT-LCAO calculations.
   J. Phys.: Conf. Ser., 2018, **1115**, 042064 (pp.1-7).
   DOI: 10.1088/1742-6596/1115/4/042064
   SNIP(2017)=0.447

5. G.A. Kaptagay, Yu.A. Mastrikov, and **E.A. Kotomin**.
   First-principles modelling of N-doped Co_3O_4.
   Latv. J. Phys. Tech. Sci., 2018, **55**, n5, pp. 36-42.
   DOI: 10.2478/lpts-2018-0034
   SNIP(2017)=0.653
6. **V.N. Kuzovkov**, **E.A. Kotomin**, and **A.I. Popov**.
   Kinetics of dimer F_2 type center annealing in MgF_2 crystals.
   Nucl. Instrum. Methods Phys. Res. B, 2018, **435**, pp. 79–82.
   DOI: 10.1016/j.nimb.2017.10.025
   SNIP(2017)=1.020, IF(2017)=1.323
7. **A. Platonenko**, **D. Gryaznov**, Yu.F. Zhukovskii, and **E.A. Kotomin**.
   Ab initio simulations on charged interstitial oxygen migration in corundum.
   Nucl. Instrum. Methods Phys. Res. B, 2018, **435**, pp. 74–78.
   DOI: 10.1016/j.nimb.2017.12.022
   SNIP(2017)=1.020, IF(2017)=1.323
8. Yu.A. Mastrikov, M.N. Sokolov, S. Koch, Yu.F. Zhukovskii, A. Gopejenko, P.V. Vladimirov, V.A. Borodin, **E.A. Kotomin**, and A. Möslang.

Ab initio modelling of the initial stages of the ODS particle formation process.
Nucl. Instrum. Methods Phys. Res. B, 2018, **435**, pp. 70–73.
DOI: 10.1016/j.nimb.2018.01.022
SNIP(2017)=1.020, IF(2017)=1.323

9. A. Lushchik, S. Dolgov, E. Feldbach, R. Pareja, **A.I. Popov**, E. Shablonin, and V. Seeman.
Creation and thermal annealing of structural defects in neutron-irradiated $MgAl_2O_4$ single crystals.
Nucl. Instrum. Methods Phys. Res. B, 2018, **435**, pp. 31–37.
DOI: 10.1016/j.nimb.2017.10.018
SNIP(2017)=1.020, IF(2017)=1.323
10. Yu.A. Mastrikov, M.N. Sokolov, **E.A. Kotomin**, A. Gopejenko, and Yu.F. Zhukovskii.
Ab initio modeling of Y and O solute atom interaction in small clusters within the bcc iron lattice.
Phys. Status Solidi B, 2018, **255**, 1800346 (pp. 1-5).
DOI: 10.1002/pssb.201800346
SNIP(2017)=0.786, IF(2017)=1.729
11. **A. Platonenko**, **D. Gryaznov**, Yu.F. Zhukovskii, and **E.A. Kotomin**.
First principles simulations on migration paths of oxygen interstitials in $MgAl_2O_4$.
Phys. Status Solidi B, 2018, **255**, 1800282 (pp. 1-7).
DOI: 10.1002/pssb.201800282
SNIP(2017)=0.786, IF(2017)=1.729
12. D. Fuks, **D. Gryaznov**, **E.A. Kotomin**, **A. Chesnokov**, and J. Maier.
Dopant solubility in ceria: alloy thermodynamics combined with the DFT+U calculations.
Solid State Ionics, 2018, **325**, pp. 258–264.
DOI: 10.1016/j.ssi.2018.08.019
SNIP(2017)=0.952, IF(2017)=2.751
13. M.F. Hoedl, E. Makagon, I. Lubomirsky, R. Merkle, **E.A. Kotomin**, and J. Maier.
Impact of point defects on the elastic properties of $BaZrO_3$: comprehensive insight from experiments and ab initio calculations.
Acta Mater., 2018, **160**, pp. 247-256.
DOI: 10.1016/j.actamat.2018.08.042
SNIP(2017)=2.737, IF(2017)=6.036
14. S. Piskunov, I. Isakoviča, and **A.I. Popov**.
Electronic structure of Mn_{Al}^{3+}- and Mn_{Al}^{2+}-doped $YAlO_3$: Prediction from the first principles.
Opt. Mater., 2018, **85**, pp. 162-166.
DOI: 10.1016/j.optmat.2018.08.039
SNIP(2017)=1.055, IF(2017)=2.320
15. Yu.A. Mastrikov, R. Merkle, **E.A. Kotomin**, M.M. Kuklja, and J. Maier.
Surface termination effects on the oxygen reduction reaction rate at fuel cell cathodes.
J. Mater. Chem. A, 2018, **6**, pp. 11929–11940.
DOI: 10.1039/c8ta02058b
SNIP(2017)=1.550, IF(2017)=9.931
16. **O. Dumbrajs** and G.S. Nusinovich.
Efficiency of gyrotrons with a tapered magnetic field in the regime of soft self-excitation.
Phys. Plasmas, 2018, **25**, 013121 (pp. 1-7).
DOI: 10.1063/1.5019974

SNIP(2017)=0.682, IF(2017)=1.941

17. **G. Zvejnieks**, A. Anspoks, **E.A. Kotomin**, and **V.N. Kuzovkov**.
Kinetic Monte Carlo modeling of Y_2O_3 nano-cluster formation in radiation resistant matrices.
Nucl. Instrum. Methods Phys. Res. B, 2018, **434**, pp. 13-22.
DOI: 10.1016/j.nimb.2018.08.005
SNIP(2017)=1.020, IF(2017)=1.323
18. S. Piskunov, I. Isakoviča, and **A.I. Popov**.
Atomic structure of manganese-doped yttrium orthoaluminate.
Nucl. Instrum. Methods Phys. Res. B, 2018, **434**, pp. 6-8.
DOI: 10.1016/j.nimb.2018.07.037
SNIP(2017)=1.020, IF(2017)=1.323
19. R.I. Eglitis and **A.I. Popov**.
Ab initio calculations for the polar (001) surfaces of $YAlO_3$.
Nucl. Instrum. Methods Phys. Res. B, 2018, **434**, pp. 1-5.
DOI: 10.1016/j.nimb.2018.07.032
SNIP(2017)=1.020, IF(2017)=1.323
20. A. Gopejenko, Yu.A. Mastrikov, Yu.F. Zhukovskii, **E.A. Kotomin**, P.V. Vladimirov, and A. Möslang.
Ab initio modelling of the Y, O, and Ti solute interaction in fcc-Fe matrix.
Nucl. Instrum. Methods Phys. Res. B, 2018, **433**, pp. 106-110.
DOI: 10.1016/j.nimb.2018.07.033
SNIP(2017)=1.020, IF(2017)=1.323
21. **A.I.Popov**, A. Lushchik, E. Shablonin, E. Vasil'chenko, **E.A. Kotomin**, **A.M. Moskina**, and **V.N. Kuzovkov**.
Comparison of the F-type center thermal annealing in heavy-ion and neutron irradiated Al_2O_3 single crystals.
Nucl. Instrum. Methods Phys. Res. B, 2018, **433**, pp. 93-97.
DOI: 10.1016/j.nimb.2018.07.036
SNIP(2017)=1.020, IF(2017)=1.323
22. A.V. Uklein, V.V. Multian, G.M. Kuz'micheva, R.P. Linnik, V.V. Lisnyak, **A.I. Popov**, and V.Ya. Gayvoronsky.
Nonlinear optical response of bulk ZnO crystals with different content of intrinsic defects.
Opt. Mater., 2018, **84**, pp. 738-747.
DOI: 10.1016/j.optmat.2018.08.001
SNIP(2017)=1.055, IF(2017)=2.320
23. M. Golub, **L.L. Rusevich**, K-D. Irrgang, and J. Pieper.
Rigid versus flexible protein matrix: light-harvesting complex II exhibits a temperature-dependent phonon spectral density.
J. Phys. Chem. B, 2018, **122**, pp. 7111–7121.
DOI: 10.1021/acs.jpcb.8b02948
SNIP(2017)=1.015, IF(2017)=3.146
24. **E. Klotins**.
Finding electron-hole interaction in quantum kinetic framework.
Latv. J. Phys. Tech. Sci., 2018, **55**, n3, pp. 43-53.
DOI: 10.2478/lpts-2018-0020
SNIP(2017)=0.653
25. A. Lushchik, Ch. Lushchik, E. Vasil'chenko, and **A.I. Popov**.
Radiation creation of cation defects in alkali halide crystals: Review and today's

concept.
Low Temp. Phys., 2018, **44**, pp. 269-277.
DOI: 10.1063/1.5030448
SNIP(2017)=0.522, IF(2017)=0.860

26. V. Serga, M. Maiorov, A. Cvetkovs, A. Krumina, and **A.I. Popov**.
Fabrication and characterization of magnetic FePt nanoparticles prepared by extraction–pyrolysis method.
Chemija, 2018, **29**, pp. 107–111.
SNIP(2017)=0.289, IF(2017)=0.394
27. R.A. Evarestov, **A. Platonenko**, and Yu.F. Zhukovskii.
Site symmetry approach applied to the supercell model of $MgAl_2O_4$ spinel with oxygen interstitials: *Ab initio* calculations.
Comput. Mater. Sci., 2018, **150**, pp. 517-523.
DOI: 10.1016/j.commatsci.2018.04.007
SNIP(2017)=1.251, IF(2017)=2.530
28. R.I. Eglitis and **A.I. Popov**.
Systematic trends in (001) surface *ab initio* calculations of ABO_3 perovskites.
J. Saudi Chem. Soc., 2018, **22**, pp. 459-468.
DOI: 10.1016/j.jscs.2017.05.011
SNIP(2017)=1.422, IF(2017)=2.456
29. **O. Dumbrajs** and T. Idehara.
Theoretical study on the 1.185-THz third harmonic gyrotron.
J. Infrared, Millimeter, Terahertz Waves, 2018, **39**, pp. 177–182.
DOI: 10.1007/s10762-017-0459-x
SNIP(2017)=1.367, IF(2017)=1.677
30. Ya. Zhydachevskyy, N. Martynyuk, **A.I. Popov**, D. Sugak, P. Bilski, S. Ubizskii, M. Berkowski, and A. Suchocki.
Theoretical study on the 1.185-THz YAP nanoceramics.
J. Phys.: Conf. Ser., 2018, **987**, 012009 (pp. 1-3).
DOI: 10.1088/1742-6596/987/1/012009
SNIP(2017)=0.447
31. **V.N. Kuzovkov**, **E.A. Kotomin**, and **A.I. Popov**.
Kinetics of the electronic center annealing in Al_2O_3 crystals.
J. Nucl. Mater., 2018, **502**, pp. 295-300.
DOI: 10.1016/j.jnucmat.2018.02.022
SNIP(2017)=1.380, IF(2017)=2.447
32. **E. Kotomin**, **V. Kuzovkov**, **A.I. Popov**, J. Maier, and R. Vila.
Anomalous kinetics of diffusion-controlled defect annealing in irradiated ionic solids.
J. Phys. Chem. A, 2018, **122**, pp. 28–32.
DOI: 10.1021/acs.jpca.7b10141
SNIP(2017)=0.964, IF(2017)=2.836
33. E. Butanovs, **J. Butikova**, A. Zolotarjovs, B. Polyakov
Towards metal chalcogenide nanowire-based colour-sensitive photodetectors
Optical Materials, 2018, **75** (pp. 501-507)
DOI: 10.1016/j.optmat.2017.11.010
SNIP(2017)=1.055, IF(2017)=2.320
34. S. Vlassov, S. Oras, M. Antsov, **J. Butikova**, R. Lõhmus, B. Polyakov
Low-friction nanojoint prototype
Nanotechnology, 2018, **29**, 195707
DOI: 10.1088/1361-6528/aab163

SNIP(2017)= 0.788, IF(2017)=3.040

35. E. Butanovs, S. Vlassov, A. Kuzmin, S. Piskunov, **J. Butikova**, B. Polyakov
Fast-Response Single-Nanowire Photodetector Based on ZnO/WS2 Core/Shell Heterostructures
ACS Applied Materials and Interfaces, 2018, **10**(16) (pp. 13869-13876)
DOI: 10.1021/acsami.8b02241
SNIP(2017)= 1.543, IF(2017)= 8.097
36. **Raitis Grzibovskis, Aivars Vembris**,
Energy level determination in bulk heterojunction systems using photoemission yield spectroscopy: case of P3HT:PCBM,
Journal of Materials Science Vol. 53, Issue 10, 7506–7515 , 2018
DOI: 10.1007/s10853-018-2050-9
SNIP(2017)= 1.06
37. Mary Robert Garrett, María Jesús Durán-Peña, William Lewis, **Kaspars Pudzs, Jānis Užulis, Igors Mihailovs**, Björk Tyril, Jonathan Shine, Emily F. Smith, **Martins Rutkis** and Simon Woodward
Synthesis and thermoelectric properties of 2- and 2,8-substituted tetrathiotetracenes.
J. Mater. Chem. C, 2018,6, 3403-3409 .
https://doi.org/10.1039/C8TC00073E
SNIP(2017)= 1.30
38. **Arturs Bundulis, Edgars Nitiss, Janis Busenbergs, Martins Rutkis**,
Mach-Zehnder interferometer implementation for thermo-optical and Kerr effect study,
Applied Physics B 124(4) , (2018),
https://doi.org/10.1007/s00340-018-6926-9
SNIP(2017)= 0.95
39. **Raitis Grzibovskis,** Aivars Vembris, Armands Sebris, Zigfrids Kapilinskis, Maris Turks,
Energy level determination of purine containing blue light emitting organic compounds, *Proc. of SPIE*, Vol. 10687, 106871D (2018)
doi: 10.1117/12.2307422
SNIP(2017)= 0.335
40. **Julija Pervenecka,** Aivars Vembris, Elmars Zarins, Valdis Kokars,
Optical and amplified spontaneous emission of neat films containing 2-cyanoacetic derivatives,
Proc. of SPIE, Vol. 10687, 1068714 (2018)
https://doi.org/10.1117/12.2306738
SNIP(2017)= 0.335
41. Kaspars Traskovskis, **Aivars Vembris**; Valdis Kokars,
Solution-processable green phosphorescent iridium(III) complexes bearing 3,3,3-triphenylpropionic acid fragment for use in OLED devices,
Proc. of SPIE, Vol. 10687, 1068715 (2018)
https://doi.org/10.1117/12.2306806
SNIP(2017)= 0.335
42. Armands Ruduss, Kaspars Traskovskis, Elina Otikova, **Aivars Vembris, Raitis Grzibovskis, Marcis Lielbardis,** Valdis Kokars,
3,3'-Bicarbazole structural derivatives as charge transporting materials for use in OLED devices,
Proc. of SPIE, Vol. 10687, 1068718 (2018)
https://doi.org/10.1117/12.2306850
SNIP(2017)= 0.335

43. **Julija Pervenecka,** Aivars Vembris**,** Elmars Zarins, Valdis Kokars,
Investigation of photoluminescence and amplified spontaneous emission properties of cyanoacetic acid derivative (KTB) in PVK amorphous thin films,
Proc. of SPIE, Vol 10687, 1068717 (2018)
https://doi.org/10.1117/12.2306835
SNIP(2017)= 0.335

44. **Arturs Bundulis,** Edgars Nitiss, Martins Rutkis,
Determination of Kerr and two-photon absorption coefficients of ABI thin films,
Proc. of SPIE, Vol 10684, 1068426 (2018);
https://doi.org/10.1117/12.2307378
SNIP(2017)= 0.335

45. **Janis Latvels,** Raitis Grzibovskis, Kaspars Pudzs, Aivars Vembris**,** Dagnija Blumberga,
Photovoltaic effect in bulk heterojunction system with glass forming indandione derivative DMABI-6Ph,
Energy Procedia, Vol. 147, 573-580 (2018)
https://doi.org/10.1016/j.egypro.2018.07.073
SNIP(2017)= 0.8

46. Elmars Zarins, Toms Puciriuss, **Julija Pervenencka, Aivars Vembris**, Valdis Kokars,
Solution processable piperazine and triphenyl moiety containing nonsymmetric bis-styryl-DWK type molecular glasses with light-emitting and amplified spontaneous emission properties,
Proc. of SPIE, Vol. 10736, 1073620-1 (2018)
doi: 10.1117/12.2319850
SNIP(2017)= 0.335

47. **Edgars Nitiss,** Janis Busengergs, Andrejs Tokmakovs, Martins Rutkis,
Preparation of an Organic Waveguide Electro-optic Modulator Operating in the Visible Spectral Range,
Sensors & Transducers, Vol. 225, Issue 9, 19-24 (2018)
SNIP(2017)= 0.21

48. Elmars Zarins, Toms Puciriuss, **Julija Pervenecka, Aivars Vembris,** Valdis Kokars,
Glass-forming nonsymmetric DWK-dyes with 5,5,5-triphenylpentyl and piparazine moieties for lightamplification studies,
Journal of Photonics for Energy 8(4), 046001 (2018),
doi: 10.1117/1.JPE.8.046001.
SNIP(2017)= 0.54

49. Bezvikonnyi, O., **Gudeika, D.,** Volyniuk, D., Grazulevicius, J.V., Bagdziunas, G.,
Pyrenyl substituted 1,8-naphthalimide as a new material for weak efficiency-roll-off red OLEDs: A theoretical and experimental study,
New Journal of Chemistry 42(15), pp. 12492-12502 (2018),
doi: 10.1039/C8NJ01866A
SNIP(2017)= 0.78

50. **Yu.N. Shunin**, S. Bellucci, V.I. Gopeyenko, T. Lobanova-Shunina, A.E. Kiv, D. Fink, A. Mansharipova, R. Muhamediyev, **Yu.F. Zhukovskii**.
Nanosensor devices for CBRN-agents detection: Theory and design. — In: J. Bonča, S. Kruchinin (eds) Nanostructured Materials for the Detection of CBRN.
NATO Science for Peace and Security ***Series A: Chemistry and Biology*** **(Springer**, Dordrecht), 2018, pp. 169-184.
DOI: 10.1007/978-94-024-1304-5_13
SNIP(2017): 0.071

51. **S. Piskunov**, **Yu.F. Zhukovskii**, **M.N. Sokolov**, J. Kleperis.
Ab initio calculations of Cu_N@Graphene (0001) nanostructures for electrocatalytic applications.
Latv. J. Phys. Tech. Sci., 2018, **55**, n6, pp. 30-34.
DOI: 10.2478/lpts-2018-0041
SNIP(2017): 0.653

52. G.A. Kaptagay, **Yu.A. Mastrikov**, E.A. Kotomin, S.A. Sandibaeva, A.S. Kopenbaeva, G.O. Baitasheva, L.S. Baikadamova.
Theoretical investigations of nitrogen doping on Co_3O_4 for water dissociation catalytically activity.
J. Phys.: Conf. Ser., 2018, **1115**, 032032.
DOI: 10.1088/1742-6596/1115/3/032032
SNIP(2017): 0.447

53. **D. Bocharov**, **S. Piskunov**, **Yu.F. Zhukovskii**, R.A. Evarestov.
Ab Initio calculations on the electronic structure and photocatalytic properties of two-dimensional WS_2 (0001) nanolayers of varying thickness.
Phys. Status Solidi RRL, 2018, **12**, 1800253.
DOI: 10.1002/pssr.201800253
SNIP(2017): 1.017

54. P. Fu, R. Jia, J. Wang, **R.I. Eglitis**, H. Zhang.
3D-graphene/boron nitride-stacking material: A fundamental van der Waals heterostructure.
Chem. Res. Chin. Univ., 2018, **34**, pp. 434-439.
DOI: 10.1007/s40242-018-8075-4
SNIP(2017): 0.384

55. S. Kenmoe, **O. Lisovski**, **S. Piskunov**, **D. Bocharov**, **Yu.F. Zhukovskii**, E. Spohr.
Water adsorption on clean and defective anatase TiO_2 (001) nanotube surfaces: A surface science approach.
J. Phys. Chem. B, 2018, **122**, pp. 5432-5440.
DOI: 10.1021/acs.jpcb.7b11697
SNIP(2017): 1.015

56. **O. Lisovski**, S. Kenmoe, **S. Piskunov**, **D. Bocharov**, **Yu.F. Zhukovskii**, E. Spohr.
Validation of a constrained 2D slab model for water adsorption simulation on 1D periodic TiO_2 nanotubes.
Comput. Condens. Matt., 2018, **15**, pp. 69-78.
DOI: 10.1016/j.cocom.2017.11.004
SNIP(2017): 0.632

57. **Yu.N. Shunin**, S. Bellucci, V.I. Gopeyenko, N. Burlutskaya, T. Lobanova-Shunina, A.E. Kiv, D. Fink, A. Mansharipova, R. Muhamediyev, and **Yu.F. Zhukovskii**.
Theory and modelling of ion track-based biosensors for CBRN-agents detection in medical applications.
Nanomedicine & Nanotechnology Open Access, 2018, 3, 000132 (pp. 1-11).
DOI: 10.23880/nnoa-16000132

58. **Yu.N. Shunin**, S. Bellucci, A. Gruodis, and T. Lobanova-Shunina.
Nonregular Nanosystems: Theory and Applications.
-Lecture Notes in Nanoscale Science and Technology, No 26 (Cham, Switzerland, Springer, 2018), 412 p.
DOI: 10.1007/978-3-319-69167-1

59. V.I. Gopeyenko and **A. Gopejenko**.
Using applications and tools to visualize ab initio calculations performed in VASP. -

Chapter in a book: L.T. De Paolis and P. Bourdot (Eds.), Augmented Reality, Virtual Reality, and Computer Graphics. Lecture Notes in Computer Science (Springer International Publishing AG, Cham, Switzerland), 2018, Part I, p. 489-496.
DOI: 10.1007/978-3-319-95270-3_41

60. D. Fink, A. Kiv, L. Alfonta, García- H. Arrellano, H.G. Muñoz, J. Vacik, V. Hnatowicz, **Yu.N. Shunin**, Y. Bondaruk, A. Mansharipova, R. Mukhamediyev. Improving the design of ion track-based biosensors.
Chapter in book: J. Bonča, S. Kruchinin (Eds.), Nanostructured Materials for the Detection of CBRN (NATO Science for Peace and Security. Series A: Chemistry and Biology (Springer Science+Business Media B.V., Cham, Switzerland), 2018, p. 185-197
DOI: 10.1007/978-94-024-1304-5_14

61. **Mironova-Ulmane, N.**, Sildos, I., Vasil'chenko, E., **Chikvaidze, G.**, Skvortsova, V., Kareiva, A., Muñoz-Santiuste, J.E., Pareja, R., **Elsts, E.**, Popov, A.I.
Optical absorption and Raman studies of neutron-irradiated $Gd_3Ga_5O_{12}$ single crystals
Nuclear Instruments and Methods in Physics Research, Section B: Beam Interactions with Materials and Atoms, (2018), 435, pp. 306-312.
DOI: 10.1016/j.nimb.2018.02.006
SNIP: 1.020

62. **Grube, J., Krieke, G.**
How activator ion concentration affects spectroscopic properties on $Ba_4Y_3F_{17}$: Er3+, Yb3+, a new perspective up-conversion material
Journal of Luminescence, 203, pp. 376-384. (2018)
DOI: 10.1016/j.jlumin.2018.06.052
SNIP: 1.086

63. **A**plesnin, S.S., Udod, L.V., Sitnikov, M.N., Kretinin, V.V., Molokeev, M.S., **Mironova-Ulmane, N.**
Dipole glass in chromium-substituted bismuth pyrostannate
Materials Research Express, 5 (11), (2018) art. no. 115202, .
DOI: 10.1088/2053-1591/aaddd9
SNIP: 0.454

64. **Antuzevics, A., Kemere, M., Krieke, G.**
Multisite formation in gadolinium doped SrF_2 nanoparticles
Journal of Alloys and Compounds, (2018) 762, pp. 500-507.
DOI: 10.1016/j.jallcom.2018.05.283
SNIP: 1.403

65. **Krieke, G., Sarakovskis, A., Springis, M.**
Cubic and rhombohedral $Ba_4Lu_3F_{17}$: Er3+in transparent glass ceramics: Crystallization and upconversion luminescence
Journal of Luminescence, (2018) 200, pp. 265-273.
DOI: 10.1016/j.jlumin.2018.04.016
SNIP: 1.086

66. Shi, X., Posysaev, S., Huttula, M., **Pankratov, V.**, Hoszowska, J., Dousse, J.-C., Zeeshan, F., Niu, Y., Zakharov, A., Li, T., Miroshnichenko, O., Zhang, M., Wang, X., Huang, Z., Saukko, S., González, D.L., van Dijken, S., Alatalo, M., Cao, W.
Metallic Contact between MoS_2 and Ni via Au Nanoglue
Small, 14 (22), (2018) art. no. 1704526, . Cited 3 times.
DOI: 10.1002/smll.201704526
SNIP: 1.558

67. **Rogulis, U., Fedotovs, A., Antuzevics, A., Berzins, D.,** Zhydachevskyy, Y., Sugak,

D.
Optical detection of paramagnetic centres in activated oxyfluoride glass-ceramics
Acta Physica Polonica A, (2018) 133 (4), pp. 785-788.
DOI: 10.12693/APhysPolA.133.785
SNIP: 0.574

68. **Antuzevics, A., Rogulis, U., Fedotovs, A.,** Popov, A.I.
Crystalline phase detection in glass ceramics by EPR spectroscopy
Low Temperature Physics, 44 (4), (2018) pp. 341-345.
DOI: 10.1063/1.5030462
SNIP: 0.522

69. **Kemere, M., Rogulis, U., Sperga, J.**
Luminescence and energy transfer in Dy3+/Eu3+co-doped aluminosilicate oxyfluoride glasses and glass-ceramics
Journal of Alloys and Compounds, (2018) 735, pp. 1253-1261. Cited 11 times.
DOI: 10.1016/j.jallcom.2017.11.077
SNIP: 1.403

70. **Krieke, G., Sarakovskis, A., Springis, M.**
Upconversion luminescence of Er3 +/Yb3 + and their role in the stabilization of cubic $NaLaF_4$ nanocrystals in transparent oxyfluoride glass ceramics
Journal of Non-Crystalline Solids, (2018) 481, pp. 335-343. Cited 1 time.
DOI: 10.1016/j.jnoncrysol.2017.11.016
SNIP: 1.190

71. **Krieke, G., Sarakovskis, A., Springis, M.**
Ordering of fluorite-type phases in erbium-doped oxyfluoride glass ceramics
Journal of the European Ceramic Society(2018), 38 (1), pp. 235-243.
DOI: 10.1016/j.jeurceramsoc.2017.08.037
SNIP: 1.698

72. K.Kaprans, J.Mateuss, A.Dorondo, G.Bajars, G.Kucinskis, P.Lesnicenoks, J.Kleperis
Electrophoretically deposited α-Fe2O3 and TiO2 composite anchored on rGO with excellent cycle performance as anode for lithium ion batteries.
Solid State Ionics, Volume 319, June 2018, Pages 1-6.
doi.org/10.1016/j.ssi.2018.01.042
IF=2.751, SNIP=0.952

73. A.Šutka, M.Vanags, U.Joost, K.Šmits, J.Ruža, J.Ločs, J.Kleperis, T.Juhna
Aqueous synthesis of Z-scheme photocatalyst powders and thin-film photoanodes from earth abundant elements.
Journal of Environmental Chemical Engineering, Volume 6, Issue 2, April 2018, Pages 2606-2615.
https://doi.org/10.1016/j.jece.2018.04.003
SNIP=1.385

74. Tanel Käämbre, Martins Vanags, Rainer Pärna, Vambola Kisand, Reinis Ignatans, Janis Kleperis, Andris Šutka
Yttrium-doped hematite photoanodes for solar water splitting: Photoelectrochemical and electronic properties.
Ceramics International, Volume 44, Issue 11, 1 August 2018, Pages 13218-13225.
https://doi.org/10.1016/j.ceramint.2018.04.147
IF=3.057, SNIP=1.167

75. Liga Avotina, Davis Conka, Aigars Vitins, Elina Pajuste, Larisa Baumane, Andris Sutka, Natalija Skute, Gunta Kizane
JET Contributors, Spectrometric analysis of inner divertor materials of JET carbon and

ITER-like walls.
Fusion Engineering and Design, In press, (5 pp.)
https://doi.org/10.1016/j.fusengdes.2018.11.037
IF=1.437, SNIP=1.273

76. **Š.Svirskas**, M.Dunce, E.Birks E., A.Sternbergs, J.Banys.
Electromechanical properties of Na0.5Bi0.5TiO3-SrTiO3-PbTiO3 solid solutions.
J.Phys.Chem.Sol., 114, 94
SNIP 2017=0.82

77. **M.Dunce**, G.Krieke, E.Birks, M.Antonova, L.Eglite, J.Grube, A.Sarakovskis.
The role of disorder on Er3+ luminescence in Na1/2Bi1/2TiO3.
J.Alloys Compd., 762, 326
SNIP 2017=1.4

78. **Š.Svirskas**, V.V.Shvartsman, M.Dunce, R.Ignatans, E.Birks, T.Ostapchuk, S.Kamba, D.C.Lupasku. J.Banys.
Two-phase dielectric polar structures in 0.1NBT-0.6ST-0.3PT solid solutions.
Acta Mater., 153, 117
SNIP 2017=2.74

79. **D.Sitko**, K.Konieczny, W.Piekarczyk, P.Czaja, J.Suchanicz, M.Antonova, A.Sternberg.
Physical properties and microstructure characteristics of (1-x)$BaTiO_3$-x$CaTiO_3$ systems.
Phase Trans., 91, Issue: 9-10, 1044 (2018)
SNIP 2017=0.56

80. **J.Suchanicz**, EM.Dutkiewicz, P.Czaja, K.Kluczewska, M.Antonova, A.Sternberg.
$SrTiO_3$-doping effect on dielectric and ferroelectric behavior of $Na_{0.5}Bi_{0.5}TiO_3$ ceramics.
Ferroelectrics, 524, Issue:1, 9 (2018)
SNIP 2017=0.41

81. A.I. Burkhanov, **K. Bormanis**, V.O. Semibratov, A.V. Sopit, A. Sternberg, M. Antonova, and A. Kalvane.
Dielectric Nonlinearity and the Velocity of Ultrasonics in the Region of the Structural Phase Transition in $(K_{0.5}Na_{0.5})(Nb_{1-x}Ta_x)O_3$ Ceramics.
Bulletin of the Russian Academy of Sciences: Physics, 2018, 82, 3, 229-233.
DOI: 10.3103/S106287381803005X
SNIP 2017=0.53

82. M. Reinfelde, M. Mitkova, T. Nichol, Z.G.Ivanova, J. Teteris
Photoinduced mass transport in Ge-Se amorphous films
Chalcogenide Letters, 15 (2018) 35-43

83. A.Gerbreders, M. Reinfelde, A. Bulanovs, A. Tokmanovs, K. Traskovskis, J. Teteris, Inffluence of acid-base modifiers on photoinduced mass transport in amorphous azobenzene amino acid
Journ. of Optoelectronics and Advanced Materials, 20 (2018) 52-55.

84. J. Miķelsone, J. Teteris
Surface relief grating recording in azobenzene epoxy films
Journ. of Optoelectronics and Advanced Materials, 20 (2018) 224-228.

85. J. Teteris
Surface relief grating recording in amorphous chalcogenide and azobenzene compounds
Journ. of Optoelectronics and Advanced Materials, 20 (2018) 229-234

86. **V. Karitans**, E. Nitiss, A. Tokmakovs, and K. Pudzs.
Optical phase retrieval using four rotated versions of a single binary mask – simulation results.

Proc. SPIE, 2018, 10694, 106940C (pp. 1-7).
DOI: 10.1117/12.2311861
SNIP(2017)=0.335

87. M.Ozolinsh, O.Danilenko, J. Aispure
Time decay of illusory "the Break of the Curveball"
Perception 47(5), 569(2018)

88. **M.Ozolinsh**, J.Aišpure, O.Danilenko, and P. Paulins.
Testing of display color causing excitation in eye periphery creating nonlinear distortions of psychophysical response.
Proc. SPIE, 2018, 10820, 108201I (pp. 1-7).
DOI: 10.1117/12.2500570
SNIP(2017)=0.335

89. **Z.Jansone, M.Ozolinsh.**
Colour Vision Sensitivity Changes Before and After Cataract Surgery.
Perception, 2018, 47(5), p.564-565.
DOI:10.1177/0301006618756416
IF(2017)=0.619

90. **M. Ozolinsh**, J.Berzinsh, A.Pastare, P.Paulins, and Z.Jansone.
Tunable liquid lens equipped virtual reality adapter for scientific, medical, and therapeutic goals.
Proc. SPIE, 2018, 10817, 1081704 (pp. 1-7).
DOI: 10.1117/12.2500292
SNIP(2017)=0.335

91. E. J.Timoshenko, A.Anspoks, A.Cintins, A.Kuzmin, **J.Purans,** A.I.Frenkel,
Neural Network Approach for Characterizing Structural Transformations by X-Ray Absorption Fine Structure Spectroscopy,
Phys. Rev. Lett. 120 (2018) 225502.
DOI: 10.1103/PhysRevLett.120.22550
SNIP (2017)=2.46

92. D. Pazos, A. Cintins, V. De Castro, P. Fernández, J. Hoffmann, W. García-Vargas, T. Leguey, **J. Purans**, A. Anspoks, A. Kuzmin, I. Iturriza, N. Ordás,
ODS ferritic steels obtained from gas atomized powders through the STARS processing route: Reactive synthesis as an alternative to mechanical alloying,
Nucl. Mater. Energy 17 (2018) 1-8.
DOI: 10.1016/j.nme.2018.05.005
SNIP (2017)=1.35

108. T. Gräning, M. Rieth, A. Möslang, A. Kuzmin, A. Anspoks, J. Timoshenko, A. Cintins, **J. Purans**
Investigation of precipitate in an austenitic ODS steel containing a carbon-rich process control agent,
Nucl. Mater. Energy 15 (2018) 237-243.
DOI: 10.1016/j.nme.2018.05.005
SNIP(2017)=1.35

109. N. Ordás, E. Gil, A. Cintins, V. de Castro, T. Leguey, I. Iturriza, **J. Purans**, A. Anspoks, A. Kuzmin, A. Kalinko,
The role of yttrium and titanium during the development of ODS ferritic steels obtained through the STARS route: TEM and XAS study,
J. Nucl. Mater. 504 (2018) 8-22.
DOI: 10.1016/j.jnucmat.2018.03.020
SNIP(2017)=1.35

110. **S. Vlassov**, S. Oras, M. Antsov, I. Sosnin, B. Polyakov, A. Shutka, M.Y. Krauchanka, L.M. Dorogin.
Adhesion and mechanical properties of PDMS-based materials probed with *AFM: A review*
SNIP(2017)=1.6

111. S. Vigonski, V. Jansson, S. Vlassov, **B. Polyakov**, E. Baibuz, S. Oras, A. Aabloo, F. Djurabekova, V. Zadin.
Au nanowire junction breakup through surface atom diffusion.
Nanotechnology. 29, Article number 015704 (2018)
DOI: 10.1088/1361-6528/aa9a1b
SNIP(2017)=0.79

112. D. Bocharov, A. Anspoks, J. Timoshenko, A. Kalinko, M. Krack, A. Kuzmin,
Interpretation of the Cu K-edge EXAFS spectra of Cu_3N using ab initio molecular dynamics,
Rad. Phys. Chem. (2018)
DOI: 10.1016/j.radphyschem.2018.12.020

113. K. Juhnevica-Radenkova, V. Radenkovs, K. Kundzins, D. Seglina,
Effect of ozone treatment on the microstructure, chemical composition and sensory quality of apple fruits,
Food Sci. Technol. Int. (2018)
DOI: 10.1177/1082013218815285

114. A. Kuzmin, J. Timoshenko, A. Kalinko, I. Jonane, A. Anspoks,
Treatment of disorder effects in X-ray absorption spectra beyond the conventional approach,
Rad. Phys. Chem. (2018)
DOI: 10.1016/j.radphyschem.2018.12.032

115. Urmas Joost, Andris Šutka, Marek Oja, Krisjanis Smits, Nicola Döbelin, Ardi Loot, Martin Järvekülg, Mika Hirsimäki, Mika Valden, and Ergo Nõmmiste
Reversible Photodoping of TiO2 Nanoparticles for Photochromic Applications
Chemistry of Materials Article ASAP
DOI: 10.1021/acs.chemmater.8b04813

116. Bite, I., Krieke, G., Zolotarjovs, A., Laganovska, K., Liepina, V., Smits, K., Auzins, K., Grigorjeva, L., Millers, D., Skuja, L.
Novel method of phosphorescent strontium aluminate coating preparation on aluminum
Materials and Design, 160, pp. 794-802.
DOI: 10.1016/j.matdes.2018.10.021

117. Grigorjeva, L., Zolotarjovs, A., Millers, D., Smits, K., Krug, P., Stollenwerk, J., Osman, A., Tenostendarp, T.
Magnetron sputtering fabrication of α-Al2O3:Cr powders and their thermoluminescence properties
Radiation Measurements, 119, pp. 140-143.
DOI: 10.1016/j.radmeas.2018.10.009

118. Laganovska, K., Bite, I., Zolotarjovs, A., Smits, K.
Niobium enhanced europium ion luminescence in hafnia nanocrystals
Journal of Luminescence, 203, pp. 358-363.
https://www.scopus.com/inward/record.uri?eid=2-s2.0-
DOI: 10.1016/j.jlumin.2018.06.069

119. Dolić, S.D., Jovanović, D.J., Smits, K., Babić, B., Marinović-Cincović, M., Porobić, S., Dramićanin, M.D.
A comparative study of photocatalytically active nanocrystalline tetragonal zyrcon-type

and monoclinic scheelite-type bismuth vanadate
Ceramics International, 44 (15), pp. 17953-17961.
DOI: 10.1016/j.ceramint.2018.06.272

120. Šutka, A., Käämbre, T., Joost, U., Kooser, K., Kook, M., Duarte, R.F., Kisand, V., Maiorov, M., Döbelin, N., Smits, K.
Solvothermal synthesis derived Co-Ga codoped ZnO diluted magnetic degenerated semiconductor nanocrystals
Journal of Alloys and Compounds, 763, pp. 164-172.
DOI: 10.1016/j.jallcom.2018.05.036

121. Gavrilović, T., Laganovska, K., Zolotarjovs, A., Smits, K., Jovanović, D.J., Dramićanin, M.D.
High resolution luminescence spectroscopy and thermoluminescence of different size LaPO4:Eu3+ nanoparticles
Optical Materials, 82, pp. 39-46.
DOI: 10.1016/j.optmat.2018.05.042

122. Kiisk, V., Puust, L., Mändar, H., Ritslaid, P., Rähn, M., Bite, I., Jankovica, D., Sildos, I., Jaaniso, R.
Phase stability and oxygen-sensitive photoluminescence of ZrO2:Eu,Nb nanopowders
Materials Chemistry and Physics, 214, pp. 135-142.
DOI: 10.1016/j.matchemphys.2018.04.090

123. Jovanović, D.J., Gavrilović, T.V., Dolić, S.D., Marinović-Cincović, M., Smits, K., Dramićanin, M.D.
Up-conversion luminescence of GdVO4:Nd3+/Er3+ and GdVO4:Nd3+/Ho3+ phosphors under 808 nm excitation
Optical Materials, 82, pp. 1-6.
DOI: 10.1016/j.optmat.2018.05.033

124. Auffray, E., Augulis, R., Fedorov, A., Dosovitskiy, G., Grigorjeva, L., Gulbinas, V., Koschan, M., Lucchini, M., Melcher, C., Nargelas, S., Tamulaitis, G., Vaitkevičius, A., Zolotarjovs, A., Korzhik, M.
Excitation Transfer Engineering in Ce-Doped Oxide Crystalline Scintillators by Codoping with Alkali-Earth Ions
Physica Status Solidi (A) Applications and Materials Science, 215 (7), art. no. 1700798
DOI: 10.1002/pssa.201700798

125. Liepina, V., Millers, D., Smits, K., Zolotarjovs, A., Bite, I.
X-ray excited luminescence of SrAl2O4:Eu,Dy at low temperatures
Journal of Physics and Chemistry of Solids, 115, pp. 381-385.
https://www.scopus.com/inward/record.uri?eid=2-s2.0-
DOI: 10.1016/j.jpcs.2017.12.040

126. Gavrilović, T., Periša, J., Papan, J., Vuković, K., Smits, K., Jovanović, D.J., Dramićanin, M.D.
Particle size effects on the structure and emission of Eu3+:LaPO4 and EuPO4 phosphors
Journal of Luminescence, 195, pp. 420-429.
DOI: 10.1016/j.jlumin.2017.12.002

127. Jovanović, D.J., Chiappini, A., Zur, L., Gavrilović, T.V., Lam Tran, T.N., Chiasera, A., Lukowiak, A., Smits, K., Dramićanin, M.D., Ferrari, M.
Synthesis, structure and spectroscopic properties of luminescent GdVO4:Dy3+ and DyVO4 particles
Optical Materials, 76, pp. 308-316.
DOI: 10.1016/j.optmat.2017.12.046

128. Vitola, V., Millers, D., Smits, K., Bite, I., Zolotarjovs, A.

The search for defects in undoped SrAl2O4 material
Optical Materials, Article in Press
DOI: 10.1016/j.optmat.2018.06.004

129. Skuja, L., Ollier, N.
Optical properties of chlorine- and oxygen-related defects in SiO2 glass and optical fibers
Optics InfoBase Conference Papers, Part F98-BGPPM 2018, 1 p.
DOI: 10.1364/BGPPM.2018.BM2A.1

130. Grigorjeva, L., Kamada, K., Nikl, M., Yoshikawa, A., Zazubovich, S., Zolotarjovs, A.
Effect of Ga content on luminescence and defects formation processes in Gd3(Ga,Al)5O12:Ce single crystals
Optical Materials, 75, pp. 331-336.
DOI: 10.1016/j.optmat.2017.10.054

131. Trukhin, A., **Antuzevics, A.**
Photoluminescence and Electron Spin Resonance of Silicon Dioxide Crystal with Rutile Structure (Stishovite)
Physica Status Solidi (A) Applications and Materials Science, Article in Press. (2018)
DOI: 10.1002/pssa.201800457
SNIP: 0.763

132. **Trinkler, L.**, Trukhnin, A., Chou, M.
Comparison of luminescence in LiGaO2, Al2O3-Ga and Al2O3-Li crystals
Latvian journal of physics and technical sciences, (2018) 6, pp. 4-12
DOI: 10.2478/lpts-2018-0038
SNIP: 0.653

133. Artyukhov, A.E., **Gabrusenoks, J.**, Rossi, P.C.
Obtaining of the modified NH_4NO_3 granules with 3-d nanoporous structure: Impact of humidifier type on the granule's structure
Springer Proceedings in Physics, (2018) 214, pp. 395-405.
DOI: 10.1007/978-3-319-92567-7_25

134. I. Jonane, A. Anspoks, A. Kuzmin,
Advanced approach to the local structure reconstruction and theory validation on the example of the W L_3-edge extended X-ray absorption fine structure of tungsten,
Modelling Simul. Mater. Sci. Eng. 26 (2018) 025004 (11 pp).
DOI: 10.1088/1361-651X/aa9bab

135. N. Mironova-Ulmane, A. Kuzmin, V. Skvortsova, G. Chikvaidze, I. Sildos, J. Grabis, D. Jankoviča, A. Dindune, M. Maiorov,
Synthesis and vibration spectroscopy of nano-sized manganese oxides,
Acta Phys. Pol. A 133 (2018) 1013-1016.
DOI: 10.12693/APhysPolA.133.1013

136. I. Jonane, A. Cintins, A. Kalinko, R. Chernikov, A. Kuzmin,
X-ray absorption near edge spectroscopy of thermochromic phase transition in $CuMoO_4$,
Low Temp. Phys. 44 (2018) 434-437.
DOI: 10.1063/1.5034155

137. C. Soto, C. García-Rosales, J. Echeberria, E. Platacis, A. Shisko, F. Muktepavela, T. Hernández, M. Malo Huerta,
Development, Characterization, and Testing of a SiC-Based Material for Flow Channel Inserts in High-Temperature DCLL Blankets,
IEEE Trans. Plasma Sci. 46 (2018) 1561-1569.

DOI: 10.1109/TPS.2018.2809571

138. A. Dauletbekova, V. Skuratov, N. Kirilkin, I. Manika, J. Maniks, R. Zabels, A. Akilbekov, A. Volkov, M. Baizhumanov, M. Zdorovets, A. Seitbayev,
Depth profiles of aggregate centers and nanodefects in LiF crystals irradiated with 34 MeV ^{84}Kr, 56 MeV ^{40}Ar and 12 MeV ^{12}C ions,
Surf. Coat. Technol. 355 (2018) 16-21.
DOI: 10.1016/j.surfcoat.2018.03.096

139. I. Manika, R. Zabels, J. Maniks, K. Schwartz, R. Grants, T. Krasta, A. Kuzmin,
Formation of dislocations in LiF irradiated with ^{3}He and ^{4}He ions,
J. Nucl. Mater. 507 (2018) 241-247.
DOI: 10.1016/j.jnucmat.2018.05.005

140. I. Jonane, A. Cintins, A. Kalinko, R. Chernikov, A. Kuzmin,
Probing the thermochromic phase transition in $CuMoO_4$ by EXAFS spectroscopy,
Phys. Status Solidi B 255 (2018) 1800074:1-5.
DOI: 10.1002/pssb.201800074

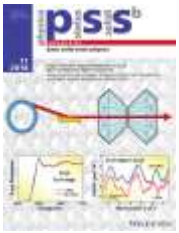

141. A. Kuzmin, A. Anspoks, A. Kalinko, J. Timoshenko, L. Nataf, F. Baudelet, T. Irifune,
Origin of pressure-induced metallization in Cu_3N: an X-ray absorption spectroscopy study,
Phys. Status Solidi B 255 (2018) 1800073:1-6.
DOI: 10.1002/pssb.201800073

142. E. I. Gorokhova, S. B. Eron'ko, E. A. Oreshchenko, A. V. Sandulenko, P. A. Rodnyĭ, K. A. Chernenko, I. D. Venevtsev, A. M. Kul'kov, F. Muktepavela, P. Boutachkov,
Structural, optical, and luminescence properties of ZnO:Ga optical scintillation ceramic,
J. Opt. Technol. 85 (2018) 729-737.
DOI: 10.1364/JOT.85.000729

143. A. Akilbekov, A. Dauletbekova, N. Kirilkin, R. Zabels, M. Baizhumanov, A. Seitbayev, Zh. Karipbayev, Sh. Giniyatova,
Luminescence of F_2 and F_3^+ centres in LiF crystals irradiated with 12 MeV ^{12}C ions,
J. Phys.: Conf. Ser. 1115 (2018) 052002.
DOI: 10.1088/1742-6596/1115/5/052002

144. A. Kuzmin, A. Anspoks, L. Nataf, F. Baudelet, T. Irifune,
Influence of pressure and temperature on X-ray induced photoreduction of nanocrystalline CuO,
Latvian J. Phys. Tech. Sci. 55(6) (2018) [in press].

145. F. Muktepavela, J. Maniks, L.Grigorjeva, P. Rodnyi, E. Gorokhova,
Effect of In doping on the ZnO powders morphology and microstructure evolution of ZnO:In ceramics as a material for scintillators,
Latvian J. Phys. Tech. Sci. 55(6) (2018) [in press].

Theses

Doctor Theses

No.	Author	Title	Supervisor	Degree
1.	**Mārtiņš Zubkins**	*Development of transparent conducting ZnO based films deposition process and films characterization*	Dr. habil. phys. **Juris Purans**	Dr. Phys.
2.	**Jelena Mikelsone**	*Holographic recording and surface relief grating formation in azobenzene compounds*	Dr. phys. **Janis Teteris**	Dr. Phys.

M.Sc. Theses

No.	Author	Mark	Title	Supervisor
1.	**Laura Eglīte**	10	Grain growth in Na0.5Bi0.5TiO3 based solid solutions	**Ēriks Birks** Dr. Phys.
2.	**Baiba Gūtmane**	9	Research and Application of Four Wave Mixing Effect in WDM-PON Access Systems	**Edgars Elsts,** Dr. phys.

B.Sc. Theses

No.	Author	Mark	Title	Supervisor
1.	**Krišjānis Auziņš**	9	*Production of phosphorescent coatings using plasma electrolytic oxidation method*	**Krišjānis Šmits Dr. phys.**
2.	**Jānis Čipa**	8	*X-ray induced effects in lithium orthosilicate pebbles with addations of lithium metatitanate*	**Aleksejs Zolotarjovs M.Sc.**
3.	**Kārlis Jirgensons**	8	*Upconversion luminescence in erbium doped $NaYF_4$*	**Anatolijs Šarakovskis Dr.phys.**
4.	**Mārcis Lielbārdis**	9	*Determination of charge carrier mobilities in organic thin films containing carbazol groups*	Aaivars Vembris Dr.phys.

5.	**Ingars Lukoševičs**	8	*Fabrication and study on applications in gas sensors of few layer graphene coating*	Jānis. Kleperis Dr.phys.
6.	**Dace Ņilova**	8	*Ultrasonic exfoliation of transition metal dichalcogenide microcrystals and characterization of their photoelectric properties*	Edgars Butanovs M.Sc.
7.	**Elīna Pavlovska**	10	*Luminescence of erbium doped barium lutetium fluoride and its dependence from temperature and erbium concentration*	Jurģis Grūbe Dr.phys.
8.	**Jānis Užulis**	9	*Studies of Thermoelectrical Properties of Tetrathiotetracene derivative thin films*	Kaspars Pudžs M.Sc.
9.	**Dāvis Zavickis**	9	*Nanoparticle defect aggregation studies in 2D iron lattice – kinetic Monte Carlo simulations*	Guntars Zvejnieks Dr.phys.
10.	**Artūrs Kalašņiks**	7	*FTIR analysis of impurities in FZ silicon single crystals grown by different technologies*	Georgijs Čikvaidze Dr.phys.